Extreme events for fractional Brownian motion with drift: Theory and numerical validation

Maxence Arutkin,[1] Benjamin Walter,[2] and Kay Jörg Wiese[3]
[1]*UMR CNRS 7083 Gulliver, ESPCI Paris, 10 rue Vauquelin, 75005 Paris, France*
[2]*Department of Mathematics, Imperial College London, London SW7 2AZ, United Kingdom*
[3]*Laboratoire de Physique de l'Ecole Normale Supérieure, ENS, Université PSL, CNRS, Sorbonne Université, Université Paris-Diderot, Sorbonne Paris Cité, 24 rue Lhomond, 75005 Paris, France*

(Received 13 October 2019; revised 21 February 2020; accepted 30 June 2020; published 4 August 2020)

We study the first-passage time, the distribution of the maximum, and the absorption probability of fractional Brownian motion of Hurst parameter H with both a linear and a nonlinear drift. The latter appears naturally when applying nonlinear variable transformations. Via a perturbative expansion in $\varepsilon = H - 1/2$, we give the first-order corrections to the classical result for Brownian motion analytically. Using a recently introduced adaptive-bisection algorithm, which is much more efficient than the standard Davies-Harte algorithm, we test our predictions for the first-passage time on grids of effective sizes up to $N_{\text{eff}} = 2^{28} \approx 2.7 \times 10^8$ points. The agreement between theory and simulations is excellent, and by far exceeds in precision what can be obtained by scaling alone.

DOI: 10.1103/PhysRevE.102.022102

I. INTRODUCTION

Understanding the extreme-value statistics of random processes is important in a variety of contexts. Examples are records [1], e.g., in climate change [2], equivalent to depinning [3], in quantitative trading [4], or for earthquakes [5]. While much is known for Markov processes, and especially for Brownian motion [6–12], much less is known for correlated, i.e., non-Markovian processes, of which fractional Brownian motion (fBm) is the simplest scale-free version [13–20].

FBm is important as it successfully models a variety of natural processes [21]: a tagged particle in single-file diffusion ($H = 0.25$) [22,23], the integrated current in diffusive transport ($H = 0.25$) [24], polymer translocation through a narrow pore ($H \simeq 0.4$) [25–27], anomalous diffusion [28], values of the log return of a stock ($H \simeq 0.6$ to 0.8) [14,29–31], hydrology ($H \simeq 0.72$ to 0.87) [32], a tagged monomer in a polymer ($H = 0.25$) [33], solar flare activity ($H \simeq 0.57$ to 0.86) [34], the price of electricity in a liberated market ($H \simeq 0.41$) [35], telecommunication networks ($H \simeq 0.78$ to 0.86) [36], telomeres inside the nucleus of human cells ($H \simeq 0.18$ to 0.35) [37], or diffusion inside crowded fluids ($H \simeq 0.4$) [38].

Recently, first-passage times of fBm have been investigated [39–44]. Due to the non-Markovian nature of the process, translating these results to a fBM with drift is far from trivial, and even properly estimating the drift for $H < 1/2$ is a challenge [45]. To our knowledge, no anaytical result for a fBm with drift are known. It is this gap we intend to fill here.

As is discussed later, apart from a *linear drift*, a *nonlinear drift* may appear as well, leading us to consider the process,

$$z_t := x_t + \mu t + \nu t^{2H}. \tag{1}$$

Here x_t is a standard fractional Brownian motion (fBm) with mean and variance

$$\langle x_t \rangle = x_0 = 0, \tag{2}$$

$$\langle x_{t_1} x_{t_2} \rangle = |t_1|^{2H} + |t_2|^{2H} - |t_1 - t_2|^{2H}. \tag{3}$$

The parameter H is the Hurst parameter. Since fBm is a Gaussian process, the above equations uniquely and completely specify it. Taking a derivative w.r.t. both t_1 and t_2 shows that the increments of the process are correlated,

$$\langle \dot{x}_{t_1} \dot{x}_{t_2} \rangle = 2H(2H-1)|t_1 - t_2|^{2H-2}. \tag{4}$$

Correlations are positive for $H > 1/2$, and negative for $H < 1/2$. The case $H = 1/2$ corresponds to Brownian motion, with uncorrelated increments.

The parameters μ and ν are the strength of linear and nonlinear drift. While linear drift is a canonical choice, nonlinear drift appears as a consequence of nonlinear variable transformations. As an example, consider the process

$$y_t := e^{z_t}. \tag{5}$$

The exponential transformation appears quite often, be it in the Black-Sholes theory of the stock market where the logarithm of the portfolio price is treated as a random walk [30,46,47], be it in nonlinear surface growth of the Kardar-Parisi-Zhang universality class [48–50], where the transformation is known as the Cole-Hopf transformation [51,52], or in the evaluation of the Pickands constant [53–60]. Like any nonlinear transform, this generates an effective drift known from Itô-calculus. Computing the average of y_t gives

$$\begin{aligned}\langle y_t \rangle = \langle e^{z_t} \rangle &= \exp\left(\langle z_t \rangle + \tfrac{1}{2}\left[\langle z_t^2 \rangle - \langle z_t \rangle^2\right]\right) \\ &= \exp(\mu t + [\nu + 1] t^{2H}).\end{aligned} \tag{6}$$

Thus, even if initially there is no nonlinear drift, it is generated by nonlinear transformations. For this reason, we include it into our model.

While for Brownian motion, equivalent to $H = \frac{1}{2}$, many results can be obtained analytically [6–12], for fBm much less is known. Recently, some of us developed a framework [61] for a systematic expansion in

$$\varepsilon := H - \tfrac{1}{2}. \tag{7}$$

It has since successfully been applied to obtain the distribution of the maximum and minimum of an fBm [42,44], to fBm bridges [62], evaluation of the Pickands constant [54], the two-sided exit problem [63] and the generalization of the three classical arcsine laws [64]. It is also known that the fractal dimension of the record set of an fBm is $d_{\mathrm{f}} = H$ [65].

This article is organized into four sections, the introduction, theory in Sec. II, and numerics in Sec. III, followed by conclusions in Sec. IV.

II. THEORY

In this section, we find the probability distribution of first-passage times and running maxima of fBm with linear and nonlinear drift by way of a perturbation expansion around simple Brownian motion. The key result of this section is the scaling function Eq. (91) which together with the auxiliary functions defined in Eqs. (94), (101), and (105) gives the distribution of first-passage times. The majority of this section is devoted to deriving these results.

A. Scaling dimensions

Before developing the perturbation theory, we consider the scaling dimensions involved. This will be useful for later discussion of the scaling functions. For fBm as defined in Eq. (1), there are four dimension-full quantities, x, t, μ, and ν. Scaling functions will thus depend on three scaling variables, which we now identify. We start with the terms without drift:

$$x \sim t^H \iff t \sim x^{\frac{1}{H}}, \tag{8}$$

where the tilde means "same scaling dimension." Thus (without drift), any observable $\mathfrak{O}(x,t)$ can be written as

$$\mathfrak{O}(x,t) = x^{\dim_x(\mathfrak{O})} f_{\mathfrak{O}}(y), \quad y := \frac{x}{\sqrt{2}t^H}. \tag{9}$$

The variable y is dimension free. In presence of a linear drift, one has

$$x \sim \mu t \iff \mu \sim \frac{x}{t} \sim x^{1-\frac{1}{H}} \sim t^{H-1}. \tag{10}$$

Thus, the combination $u = \mu x^{\frac{1}{H}-1}$ is dimension free, as is $\tilde{u} := u^{\frac{H}{1-H}} = \mu^{\frac{H}{1-H}} x$. For nonlinear drift, we have

$$x \sim \nu t^{2H} \iff \nu \sim \frac{x}{t^{2H}} \sim \frac{1}{x} \sim \frac{1}{t^H}. \tag{11}$$

Another scaling variable therefore is $v = \nu x$. In conclusion, any observable $\mathcal{O}$ can, in generalization of Eq. (9), be written as

$$\mathfrak{O}(x,t,\mu,\nu) = x^{\dim_x(\mathfrak{O})} f_{\mathfrak{O}}(y,u,v), \tag{12}$$

$$y = \frac{x}{\sqrt{2}t^H}, \tag{13}$$

$$u = \mu x^{\frac{1}{H}-1}, \quad \text{or} \quad \tilde{u} = \mu^{\frac{H}{1-H}} x, \tag{14}$$

$$v = \nu x. \tag{15}$$

TABLE I. Notations used for probabilities and their various densities.

P	Probability
$P = \partial_x \mathbf{P}$	Probability density in x
$\mathbb{P} = \partial_t \mathbf{P}$	Probability density in t
$\mathcal{P} = \partial_y \mathbf{P}$	Probability density in y

B. The first-passage time

The central result of our work is a perturbative expression of the first-passage-time density of fBM with linear and nonlinear drift as introduced in Eq. (1). The first-passage time t_{FP} is defined as

$$t_{\mathrm{FP}}(m) := \inf_{t>0} \{t, z_t \leqslant 0 | z_{t=0} = m\}, \tag{16}$$

where m is the starting point of the process z_t, and $m > 0$. The first-passage-time density for Brownian motion with (linear) drift, see, e.g., Ref. [6], and rederived below in Eq. (30), is

$$\mathbb{P}_0(t_{\mathrm{FP}}(m) = t) = \frac{m}{2\sqrt{\pi}t^{3/2}} e^{-\frac{1}{2}\left(\frac{m}{\sqrt{2t}} + \frac{\mu}{2}\sqrt{2t}\right)^2}. \tag{17}$$

This density in time is most naturally expressed in terms of the scaling variable y introduced in Eq. (9), and which for Brownian motion ($H = 1/2$) reads

$$y = \left.\frac{m}{\sqrt{2t}}\right|_{t=t_{\mathrm{FP}}(m)}. \tag{18}$$

For Brownian Motion the probability distribution of y takes the simple form

$$\mathcal{P}_0(y;\mu) = \sqrt{\frac{2}{\pi}}\, e^{-\mathcal{F}_0(y;\mu)}, \tag{19}$$

$$\mathcal{F}_0(y;\mu) = \frac{1}{2}\left(y + \frac{\mu}{2}\frac{m}{y}\right)^2. \tag{20}$$

Note that the measure is dt in Eq. (17) (density in time), whereas in Eq. (19) it is dy (density in y). To avoid confusion, we use distinct symbols for probabilities **P**, densities $\mathbb{P}$ in time t, densities $\mathcal{P}$ in y, and densities P in space x, independent of the actual choice of variables. This is summarized in Table I.

We introduced the scaling function $\mathcal{F}_0$. Below we compute its corrections to first order in ε, leading to a correction of the first-passage density in y,

$$\mathcal{P}(y;\mu,\nu) = \frac{y^{\frac{1}{H}-2}}{\sqrt{2\pi}H} e^{-\mathcal{F}_0(y;\mu,\nu) - \varepsilon\delta\mathcal{F}(y;\mu,\nu)} + \mathcal{O}(\varepsilon^2). \tag{21}$$

The result is given in Eqs. (90) and (91). Two comments are in order: (i) the exponential resummation is chosen for

better convergence for larger ε, as discussed in Ref. [63], Sec. IV.C; (ii) the distribution of first-passage times is related to the distribution of maxima.

Readers wishing to skip ahead will find the function $\delta\mathcal{F}$ evaluated using path-integral methods, described in Sec. II E. For the explicit result, see Sec. II L. A confirmation by numerical simulations is shown in Sec. III B.

C. Summary of calculations to be done

To calculate the first-passage-time distribution, we consider the process $z_t > 0$ in the presence of an absorbing boundary condition at $z = 0$ and restrict ourselves to $z_t > 0$. The transition probability density of the process z_t to pass from $z_0 > 0$ to $z_1 > 0$ in time t, without being absorbed at $z = 0$ is denoted $P_+^{\mu,\nu}(z_0, z_1; t)$. The probability density of first-passage times $\mathbb{P}(t_{\rm FP}(m) = t)$ can then be obtained as

$$\mathbb{P}(t_{\rm FP}(m) = t) = \partial_{z_1} P_+^{\mu,\nu}(m, z_1, t)\big|_{z_1=0}. \tag{22}$$

This relation holds since the derivative on the right-hand side picks out those trajectories which assume $z_t = 0$ at time t for the first time. The general strategy of this work is to compute $\partial_{z_1} P_+^{\mu,\nu}(m, z_1, t)|_{z_1=0}$ and its perturbative corrections using path-integral methods. In the subsequent Sec. II D, we discuss the reference point of our expansion, simple Brownian motion. In Sec. II E, we introduce a perturbative expansion around Brownian motion, based on a path-integral formalism. This yields a diagrammatic expansion (Sec. II F), with three diagrams, listed in Sec. II G, evaluated in Secs. II H to II J, and regrouped in Sec. II K. The final result is given in Sec. II L. Contrary to the drift-free case, not all processes are absorbed, as is discussed in Sec. II M. Relations between the different probability densities are discussed in Sec. II N, followed by an analysis of the tail of these distributions in Sec. II O. Numerical checks are presented in Sec. III, followed by conclusions in Sec. IV.

D. Simple Brownian motion: First-passage time and absorption probability

The perturbation theory is an expansion around simple Brownian motion. This base point is considered here. By setting $H = \frac{1}{2}$ and $\nu = 0$ in Eq. (1), we obtain simple Brownian motion with drift. For this process, we compute (i) the positive transition probability and (ii) the absorption probability.

The transition probability of simple Brownian motion P_+^μ (to alleviate our notations, we do not put an index 0 to indicate Brownian motion, since P_+ is not used for fBm), the probability to pass from z_0 to z_1 within time t without crossing the line $z \equiv 0$, satisfies the associated Fokker-Planck equation,

$$\partial_t P_+^\mu(z_0, z_1, t) = \partial_{z_1}^2 P_+^\mu(z_0, z_1, t) - \mu\partial_{z_1} P_+^\mu(z_0, z_1, t), \tag{23}$$

with appropriate absorbing boundary condition at $z \equiv 0$. Its solution is given by the mirror-charge solution

$$P_+^\mu(z_0, z_1, t) = \frac{1}{\sqrt{4\pi t}}(e^{-(z_1-z_0)^2/4t} - e^{-(z_1+z_0)^2/4t}) \times e^{\frac{\mu}{2}(z_1-z_0)-\frac{\mu^2 t}{4}}, \tag{24}$$

satisfying the initial condition

$$P_+^\mu(z_0, z_1, t = 0) = \delta(z_0 - z_1). \tag{25}$$

It is useful to consider its Laplace-transformed version. We define the Laplace transform of a function $f(t)$, with $t \geqslant 0$ as

$$\tilde{f}(s) := \mathcal{L}_{t\to s}[f(t)] = \int_0^\infty dt\, e^{-st} f(t). \tag{26}$$

This yields

$$\tilde{P}_+^\mu(z_0, z_1, s) = e^{\frac{\mu}{2}(z_1-z_0)}\tilde{P}_+\Big(z_0, z_1, s + \frac{\mu^2}{4}\Big), \tag{27}$$

where the drift-free propagator reads

$$\tilde{P}_+(z_0, z_1, s) = \frac{e^{-\sqrt{s}(z_0-z_1)} - e^{-\sqrt{s}(z_0+z_1)}}{2\sqrt{s}}. \tag{28}$$

The Laplace transform $\tilde{\mathbb{P}}(m, s)$ of the first-passage-time probability density, following Eq. (22), equals the probability to go close to the boundary, and there being absorbed for the first time,

$$\begin{aligned}\tilde{\mathbb{P}}(m, s) &:= \int_0^\infty dt\, e^{-st}\mathbb{P}(t_{\rm FP}(m) = t)\\ &= \partial_{z_1}\tilde{P}_+^\mu(m, z_1, s)\big|_{z_1=0}\\ &= e^{-\frac{\mu}{2}m}e^{-m\sqrt{s+\mu^2/4}}.\end{aligned} \tag{29}$$

Its inverse Laplace transform is the first-passage-time probability density,

$$\mathbb{P}(t_{\rm FP}(m) = t) = e^{-\frac{\mu}{2}m-\frac{\mu^2}{4}t}\frac{me^{-\frac{m^2}{4t}}}{2\sqrt{\pi}t^{3/2}}, \tag{30}$$

confirming the result in Eq. (17). The total (time integrated) absorption probability is

$$\begin{aligned}\mathbf{P}_{\rm abs}(m) &= \tilde{\mathbb{P}}(m, s = 0)\\ &= e^{-\frac{\mu}{2}m}e^{-\frac{|\mu|}{2}m} = \begin{cases} e^{-\mu m} & , \quad \mu > 0 \\ 1 & , \quad \mu \leqslant 0 \end{cases}.\end{aligned} \tag{31}$$

In what follows, we present perturbative corrections of these results for $\varepsilon \neq 0$.

E. The path-integral of a fBm with drift

The technology developed in Refs. [42,61,63] uses a path-integral to describe fBM. Since z_t is Gaussian, its path-probability measure on a finite interval $[0, T]$ is

$$\mathbf{P}[z_t] = \exp(-\mathcal{S}[z_t; \mu, \nu]), \tag{32}$$

where $\mathcal{S}[z_t; \mu, \nu]$ is an action quadratic in z_t. Without drift ($\mu = \nu = 0$), the action for a fBM to order ε is [42,61,63]

$$\begin{aligned}&\mathcal{S}[z_t; \mu = \nu = 0]\\ &= \int_0^T dt\,\frac{\dot{z}_t^2}{4D_\varepsilon} - \frac{\varepsilon}{2}\int_\tau^T dt_2\int_0^{t_2-\tau} dt_1\frac{\dot{z}_{t_1}\dot{z}_{t_2}}{|t_1 - t_2|}.\end{aligned} \tag{33}$$

The action consists of a local part, corresponding to simple Brownian motion, and a nonlocal part, proportional to ε. The idea behind the perturbative expansion is that Brownian motion (as given by the first term) samples the whole phase space of fBm, albeit with the wrong probability measure.

Our perturbation theory corrects this, by weighing each path with the second term in Eq. (33). This implies that the absorbing boundary conditions at the origin are properly taken into account, and that observables as the absorption current, which are given by local operators, remain valid. For regularity, a short-distance cutoff $|t_1 - t_2| > \tau$ is introduced in the last integral, which is reflected in the diffusion constant [42]

$$D_\varepsilon = 2H\tau^{2H-1} = (1+2\varepsilon)\tau^{2\varepsilon} = (e\tau)^{2\varepsilon} + \mathcal{O}(\varepsilon^2). \tag{34}$$

Let us now insert the definition Eq. (1) into the action Eq. (33). The reason to proceed this way is that the method of images on which our further calculation relies works in terms of x_t as defined in Eq. (1), but not z_t. After some algebra we arrive at the action for an arbitrary drift

$$\begin{aligned}\mathcal{S}[z_t] = &\int_0^T dt\, \frac{\dot z_t^2}{4D_\varepsilon} \\ &+ \int_0^T dt \frac{\varepsilon}{2}\dot z_t\left[(\mu+\nu)\ln\left(\frac{t(T-t)}{\tau^2}\right) - 2\nu\ln\left(\frac{t}{\tau}\right)\right] \\ &- \frac{\varepsilon}{2}\int_\tau^T dt_2 \int_0^{t_2-\tau} dt_1 \frac{\dot z_{t_1}\dot z_{t_2}}{|t_1-t_2|} \\ &- \frac{z_T - z_0}{2}\left[\frac{\mu}{D_\varepsilon} + \nu\right] + \frac{T}{4}(\mu+\nu)^2 \\ &+ \frac{T}{2}\varepsilon(\nu^2-\mu^2)\ln(T) + \mathcal{O}(\varepsilon^2).\end{aligned} \tag{35}$$

Some checks are in order. In absence of absorbing boundaries, the exact free propagator reads

$$\begin{aligned}P^{\mu,\nu}(0,z,T) &= \frac{1}{2\sqrt{\pi}T^H} e^{-\frac{(z-\mu T-\nu T^{2H})^2}{4T^{2H}}} \\ &= \frac{1}{2\sqrt{\pi}T^H}\exp\left(-\frac{z^2}{4T^{2H}} + \frac{z}{2}[\nu+\mu T^{-2\varepsilon}]\right. \\ &\quad \left. - \frac{T}{4}[\nu T^{\varepsilon}+\mu T^{-\varepsilon}]^2\right).\end{aligned} \tag{36}$$

Since the above formalism has variables $\dot z$ only, the term $\sim z^2$ is given by the drift-free perturbation theory. We can further check that if we replace in the action $\dot z(t)$ by its "classical trajectory," i.e., $\dot z(t) \to [z(T) - z(0)]/T$, then both the normalization and the drift term agree with the exact propagator.

Let us specify Eq. (35) to the two cases of interest: For a fBm with *linear drift* as given in Eq. (1) with $\nu = 0$, we have

$$\begin{aligned}\mathcal{S}_{\nu=0}[z_t] = &\int_0^T dt\, \frac{\dot z_t^2}{4D_\varepsilon} - \frac{\mu}{2D_\varepsilon}(z_T - z_0) + \frac{T^{1-2\varepsilon}}{4}\mu^2 \\ &- \frac{\varepsilon}{2}\int_\tau^T dt_2 \int_0^{t_2-\tau} dt_1 \frac{\dot z_{t_1}\dot z_{t_2}}{|t_1-t_2|} \\ &+ \frac{\varepsilon\mu}{2}\int_0^T dt\, \dot z_t \ln\left(\frac{[T-t]t}{\tau^2}\right) + \mathcal{O}(\varepsilon^2).\end{aligned} \tag{37}$$

For a fBm with *nonlinear drift* as given in Eq. (1) with $\mu = 0$, we have

$$\begin{aligned}\mathcal{S}_{\mu=0}[z] = &\int_0^T dt\, \frac{\dot z_t^2}{4D_\varepsilon} - \frac{\nu}{2}(z_T - z_0) + \frac{T^{1+2\varepsilon}}{4}\nu^2 \\ &- \frac{\varepsilon}{2}\int_\tau^T dt_2 \int_0^{t_2-\tau} dt_1 \frac{\dot z_{t_1}\dot z_{t_2}}{|t_1-t_2|} \\ &+ \frac{\varepsilon\nu}{2}\int_0^T dt\, \dot z_t \ln\left(\frac{T-t}{t}\right) + \mathcal{O}(\varepsilon^2).\end{aligned} \tag{38}$$

Note the appearance of the diffusion constant in the "bias" (Girsanov) term $z_T - z_0$ for a linear drift, and its absence for a nonlinear drift.

To simplify the notation, we introduce

$$\mathcal{S}_0[z_t] = \int_0^T dt\, \frac{\dot z_t^2}{4} \tag{39}$$

as a shorthand for the Brownian action around which perturbation theory expands. The drift (Girsanov) term is $e^{-\mathcal{S}_\mathrm{d}}$, with

$$\mathcal{S}_\mathrm{d}[z] = \frac{z_0 - z_T}{2}\left(\frac{\mu}{D_\varepsilon} + \nu\right) + \frac{T}{4}(\mu T^{-\varepsilon} + \nu T^{\varepsilon})^2. \tag{40}$$

Further, define (valid at leading order in ε)

$$\alpha := \mu - \nu, \quad \beta := \mu + \nu, \tag{41}$$

$$\mu = \frac{\alpha+\beta}{2}, \quad \nu = \frac{\beta-\alpha}{2}. \tag{42}$$

This simplifies the drift terms in the action to

$$\mathcal{S}_\alpha[z_t] := \frac{1}{2}\int_0^T dt\, \dot z_t \ln\left(\frac{t}{\tau}\right), \tag{43}$$

$$\mathcal{S}_\beta[z_t] := \frac{1}{2}\int_0^T dt\, \dot z_t \ln\left(\frac{T-t}{\tau}\right). \tag{44}$$

Finally, the drift-independent perturbative correction containing the nonlocal interaction reads

$$\mathcal{S}_1[z_t] = \frac{1}{2}\int_\tau^T dt_2 \int_0^{t_2-\tau} dt_1 \frac{\dot z_{t_1}\dot z_{t_2}}{|t_1-t_2|}. \tag{45}$$

In these notations, the action to order ε reads

$$\mathcal{S}[z_t;\mu,\nu] = \frac{\mathcal{S}_0}{D_\varepsilon} + \mathcal{S}_\mathrm{d} - \varepsilon(\mathcal{S}_1 - \alpha\mathcal{S}_\alpha - \beta\mathcal{S}_\beta). \tag{46}$$

Perturbation theory takes place in the three interaction-terms proportional to ε, plus an additional contribution due to D_ε. The bare result Eq. (27) of transition probabilities of fBM will thus be corrected by three different terms corresponding to the three interaction terms $\mathcal{S}_\alpha$, $\mathcal{S}_\beta$, and $\mathcal{S}_1$, plus a correction from D_ε. The (diagrammatic) rules for computing these corrections are outlined in the next section.

F. Diagrammatic expansion

The central aim of this work is to calculate the first-passage-time density. This is done by taking the derivative of the survival transition density at its endpoint [cf. Eq. (22)]. The latter is obtained perturbatively by evaluating a

path-integral over the action defined previously:

$$\mathbb{P}^{\mu,\nu}(m,t) := \partial_{z_1} P^{\mu,\nu}_{+,\varepsilon}(m,z_1,t)\Big|_{z_1=0} \equiv \lim_{z_1\to 0}\frac{1}{z_1} P^{\mu,\nu}_{+,\varepsilon}(m,z_1,t). \quad (47)$$

Here we introduced $P^{\mu,\nu}_{+,\varepsilon}(m,z_1,t)$

$$P^{\mu,\nu}_{+,\varepsilon}(m,z_1,t) := \int_{z_0=m}^{z_t=z_1} \mathcal{D}[z_t]\Theta(z_t)\exp(-\mathcal{S}), \quad (48)$$

the probability of a path z_t to pass from m to z_1 within time t without being absorbed at $z=0$ [cf. Eq. (24)]. At first order in ε, this path integral has four perturbative contributions: The three diagrams induced by $\mathcal{S}_1$, $\mathcal{S}_\alpha$, and $\mathcal{S}_\beta$, as well as the change in the diffusion constant D_ε. The simplest way of doing these calculations is to calculate with $D=1$, and finally correct for $D_\varepsilon \neq 1$ by writing the FPT density in time of z_t as

$$\mathbb{P}^{\mu,\nu}(m,t) = \mathbb{G}^{\mu,\nu}(m,tD_\varepsilon), \quad (49)$$

where we introduce the auxiliary probability density

$$\mathbb{G}^{\mu,\nu}(m,t) = \frac{\partial}{\partial_{z_1}}\Big|_{z_1=0}\int_{z_0=m}^{z_t=z_1}\mathcal{D}[z_t]\Theta(z_t) \times e^{-\mathcal{S}^0-\mathcal{S}_{\rm d}+\varepsilon(\mathcal{S}_1-\alpha\mathcal{S}_\alpha-\beta\mathcal{S}_\beta)} + \mathcal{O}(\varepsilon^2). \quad (50)$$

We now use the perturbation expansion established in Refs. [42,44,61,62]; we refer to Refs. [42,43] for a detailed introduction, and only briefly summarize the method.

The function $\mathbb{G}^{\mu,\nu}(m,t)$ introduced above has the perturbative expansion

$$\mathbb{G}^{\mu,\nu}(m,t) = e^{-\mathcal{S}_{\rm d}}[\mathbb{G}_0(m,t) + \varepsilon\,\delta\mathbb{G}(m,t)], \quad (51)$$

where

$$\delta\mathbb{G}(m,t) = \partial_{z_1}\Big|_{z_1=0}\int_{z_0=m}^{z_t=z_1}\mathcal{D}[z_t]\Theta(z_t)\big(\mathcal{S}_1-\alpha\mathcal{S}_\alpha-\beta\mathcal{S}_\beta\big)e^{-S_0} \stackrel{!}{=} \mathbb{G}_1(m,t)-\alpha\mathbb{G}_\alpha(m,t)-\beta\mathbb{G}_\beta(m,t)+\mathcal{O}(\varepsilon). \quad (52)$$

The three auxiliary functions are defined as

$$\mathbb{G}_1(m,t) := \partial_{z_1}\int_{z_0=m}^{z_t=z_1}\mathcal{D}[z_t]\Theta(z_t)\mathcal{S}_1 e^{-S_0}\Big|_{z_1=0}, \quad (53)$$

$$\mathbb{G}_\alpha(m,t) := \partial_{z_1}\int_{z_0=m}^{z_t=z_1}\mathcal{D}[z_t]\Theta(z_t)\mathcal{S}_\alpha e^{-S_0}\Big|_{z_1=0}, \quad (54)$$

$$\mathbb{G}_\beta(m,t) := \partial_{z_1}\int_{z_0=m}^{z_t=z_1}\mathcal{D}[z_t]\Theta(z_t)\mathcal{S}_\beta e^{-S_0}\Big|_{z_1=0}. \quad (55)$$

As the term $\mathcal{S}_{\rm d}$ only depends on the initial and final point, as well as the time T, we were able to take it out. Each of the perturbations $\mathcal{S}_1$, $\mathcal{S}_\alpha$, and $\mathcal{S}_\beta$, defined in Eqs. (43)–(45) has to be evaluated inserted into the path integral with absorbing boundaries at $z=0$.

Let us summarize the rules of this perturbative expansion, explained in detail in Ref. [42]. The first step is to perform a Laplace transform, from the time variable t to the Laplace conjugate s. This transform has two advantages: First of all, it eliminates integrals over the intermediate times. Second, the propagator Eqs. (27) and (28) is exponential in the space variables, thus the latter can be integrated over.

The next step is to eliminate the denominator in Eq. (45), using a Schwinger parametrization (Eq. (31) of Ref. [42]),

$$\frac{1}{t_2-t_1} = \int_{y>0} e^{-y(t_2-t_1)}. \quad (56)$$

The variable y on the right-hand side of Eq. (56) can be interpreted as a shift in the Laplace variable s associated to the time difference t_2-t_1, i.e.,

$$s \to s+y, \quad (57)$$

for all propagators between times t_1 and time t_2. For an example see the first diagram in Eq. (65) below.

The integral over times necessitates a cutoff τ at small times, which can be replaced by a cutoff Λ for large y (Eq. (A3) of Ref. [42]). Their relation is

$$\int_0^T dt\int_0^\Lambda e^{-yt}dy = \ln(T\Lambda)+\gamma_{\rm E}+\mathcal{O}(e^{-T\Lambda}) \stackrel{!}{=} \ln\left(\frac{T}{\tau}\right) = \int_\tau^T \frac{1}{t}\,dt. \quad (58)$$

This implies the choice

$$\Lambda = e^{-\gamma_{\rm E}}/\tau. \quad (59)$$

Finally, while the insertion of the position x_t at time t with $0<t<T$ leads to a factor of x in the corresponding propagators,

$$\langle z_t\rangle_{z_0=a,z_T=b} = \int_z P_+(a,z,t)zP_+(z,b,T-t), \quad (60)$$

the insertion of $\dot{x}_t$ yields a derivative (Eq. (A1) of Ref. [42]),

$$\langle \dot{z}_t\rangle_{z_0=a,z_T=b} = 2\int_z P_+(a,z,t)\partial_z P_+(z,b,T-t). \quad (61)$$

Here $P_+(a,b,T)$ is the Brownian transition density introduced in Eq. (24) in the absence of drift ($\mu=0$).

G. Diagrams to be evaluated

The three auxiliary functions introduced in Eqs. (53)–(55) have a diagrammatic representation presented in Fig. 1. They give to first order in ε for $\mathbb{G}$,

$$\mathbb{G}^{\mu,\nu}(m,T) := \exp\left[-\frac{m}{2}\left(\frac{\mu}{D_\varepsilon}+\nu\right)-\frac{T}{4}(\mu T^{-\varepsilon}+\nu T^{\varepsilon})^2\right] \times\{\mathbb{G}_0(m,T)+\varepsilon[\mathbb{G}_1(m,T)-\alpha\,\mathbb{G}_\alpha(m,T) -\beta\mathbb{G}_\beta(m,T)]\}. \quad (62)$$

The zeroth-order contribution $\mathbb{G}_0(m,t)$ follows from Eqs. (29) and (30),

$$\mathbb{G}_0(m,t) = \frac{me^{-\frac{m^2}{4t}}}{2\sqrt{\pi}t^{3/2}}, \quad (63)$$

$$\tilde{\mathbb{G}}_0(m,s) = e^{-m\sqrt{s}}. \quad (64)$$

H. Order ε, first diagram $\mathbb{G}_1$

The Laplace transform of the first diagram is obtained from the insertion of $\mathcal{S}_1$ (without drift), as represented by the first diagram of Fig. 1, using the Brownian propagators found in Eq. (27). (The global factor of $2=2^2/2$ comes from a factor

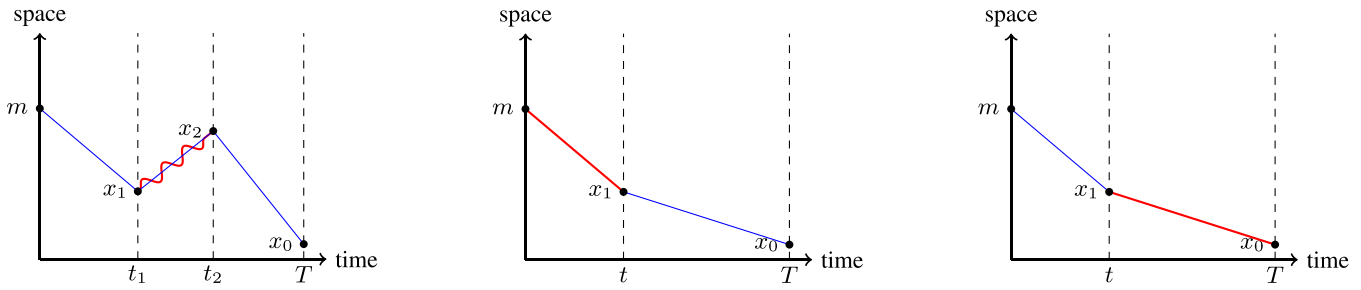

FIG. 1. Graphical representation of the path-integral for diagram $\mathbb{G}_1(m,t)$ (left, expectation of $\mathcal{S}_1$), $\mathbb{G}_\alpha(m,t)$ (middle, expectation of $\mathcal{S}_\alpha$), and $\mathbb{G}_\beta(m,t)$ (right, expectation of $\mathcal{S}_\beta$). The wiggly line in the first diagram represents the interaction proportional to $1/(t_2-t_1)$. The red lines in the second and third diagram contain a log of the corresponding time difference, $\ln(t/T)$ for the first, and $\ln[(T-t)/T]$ for the second.

of 2 for each insertion of $\dot{x}$, and the $1/2$ from the action.)

$$\begin{aligned}\tilde{\mathbb{G}}_1(m,s) &= \lim_{x_0\to 0}\frac{2}{x_0}\int_0^\Lambda dy\int_{x_1>0}\int_{x_{2>0}}\tilde{P}_+(m,x_1,s)\partial_{x_1}\tilde{P}_+(x_1,x_2,s+y)\partial_{x_2}\tilde{P}_+(x_2,x_0,s)\\ &= 2\int_0^\Lambda dy\frac{\sqrt{s}(e^{-m\sqrt{s}}(my-2\sqrt{s+y})+2\sqrt{s+y}e^{-m\sqrt{s+y}})}{2y^2}\\ &= e^{m\sqrt{s}}(m\sqrt{s}+1)\mathrm{Ei}(-2m\sqrt{s})+e^{-m\sqrt{s}}\left\{m\sqrt{s}\left[\ln\left(\frac{m}{2\sqrt{s}\tau}\right)-1\right]-\ln\left(2m\sqrt{s}\right)-\gamma_\mathrm{E}\right\},\end{aligned}\tag{65}$$

where we introduced the exponential integral function $\mathrm{Ei}(z)=-\int_{-z}^{\infty}dt\,\frac{e^{-z}}{z}$, and used Eq. (59) to eleminate Λ. For the inverse Laplace transform we find using Appendix C of Ref. [62]

$$\mathbb{G}_1(m,t)=\mathbb{G}_0(m,t)\left[\mathcal{I}\left(\frac{m}{\sqrt{2t}}\right)+2\left(\frac{m^2}{4t}-1\right)\ln\left(\frac{m^2}{\tau}\right)+\ln\left(\frac{t}{\tau}\right)+\frac{(\gamma_\mathrm{E}-1)m^2}{2t}-2\gamma_\mathrm{E}-1\right].\tag{66}$$

The special function $\mathcal{I}$ appearing in this expression was introduced in Ref. [61], Eq. (B53),

$$\mathcal{I}(z)=\frac{z^4}{6}{}_2F_2\left(1,1;\frac{5}{2},3;\frac{z^2}{2}\right)+\pi(1-z^2)\,\mathrm{erfi}\left(\frac{z}{\sqrt{2}}\right)-3z^2+\sqrt{2\pi}e^{\frac{z^2}{2}}z+2,\tag{67}$$

where $\mathrm{erfi}(z)$ is the imaginary error function. Using the definition Eq. (59) of Λ, Eq. (66), and introducing the variable

$$z:=\frac{m}{\sqrt{2t}},\tag{68}$$

$\mathbb{G}_0(m,t)$ and $\mathbb{G}_1(m,t)$ can be written more compactly as

$$t\mathbb{G}_0(m,t)=\frac{e^{-\frac{z^2}{2}}z}{\sqrt{2\pi}},\tag{69}$$

$$\begin{aligned}\mathbb{G}_1(m,t)=\mathbb{G}_0(m,t)\Bigg\{&\mathcal{I}(z)-\ln\left(\frac{4tz^4}{\tau}\right)+z^2\left[\ln\left(\frac{2tz^2}{\tau}\right)\right.\\ &\left.+\gamma_\mathrm{E}-1\right]-2\gamma_\mathrm{E}-1\Bigg\}.\end{aligned}\tag{70}$$

Note that there is a global prefactor of $1/t$, and a logarithmic dependence on t and τ.

I. Order ϵ, second diagram $\mathbb{G}_\alpha$

To study perturbations with S_α defined in Eq. (43), we represent the logarithm as

$$\ln\left(\frac{t}{\tau}\right)=\int_0^\infty\frac{dy}{y}\left[e^{-\tau y}-e^{-ty}\right].\tag{71}$$

This yields for the insertion of $\mathcal{S}_\alpha$

$$\begin{aligned}\tilde{\mathbb{G}}_\alpha(m,s) &= \lim_{x_0\to 0}\frac{1}{x_0}\int_0^\Lambda\frac{dy}{y}\int_{x_1>0}[\tilde{P}_+(m,x_1,s)e^{-\tau y}\\ &\quad-\tilde{P}_+(m,x_1,s+y)]\partial_{x_1}\tilde{P}_+(x_1,x_0,s)\\ &= \int_0^{\Lambda/s}dy\left[\frac{e^{-m\sqrt{s}}}{\sqrt{s}y^2}-\frac{e^{-m\sqrt{s}\sqrt{y+1}}}{\sqrt{s}y^2}-\frac{me^{-m\sqrt{s}-s\tau y}}{2y}\right]\\ &= \frac{1}{4}me^{-m\sqrt{s}}\left[2e^{2m\sqrt{s}}\mathrm{Ei}(-2m\sqrt{s})+\ln\left(\frac{4s\tau^2}{m^2}\right)+2\right]\\ &\quad+\mathcal{O}(\Lambda^{-1}).\end{aligned}\tag{72}$$

We checked that the y integrand is convergent, at least as $1/y^2$ for large y, and has a finite limit for $y\to 0$; thus neither x_0 nor Λ are necessary as UV cutoffs, and the y integral is finite. The τ-dependence stems from the $\ln(t/\tau)$ of the perturbation term.

Doing the inverse Laplace transform using Appendix C of Ref. [62], we get with z defined in Eq. (68)

$$\sqrt{t}\mathbb{G}_\alpha(m,t) = \frac{e^{-\frac{z^2}{2}}z^2[\mathcal{I}(z)-2]}{2\sqrt{\pi}(1-z^2)} + \frac{z\,\mathrm{erfc}(\frac{z}{\sqrt{2}})}{\sqrt{2}(z^2-1)} - \frac{e^{-\frac{z^2}{2}}z^2\big[\ln\big(\frac{2tz^2}{\tau}\big)+\gamma_\mathrm{E}-1\big]}{2\sqrt{\pi}}, \tag{73}$$

defining the complementary error function $\mathrm{erfc}(z) = 1-\mathrm{erf}(z)$. Note that there is no pole at $z=1$. Indeed, for $z\to 1$ one obtains

$$\frac{-{}_2F_2\big(1,1;\frac{5}{2},3;\frac{1}{2}\big) - 4\,{}_2F_2\big(1,1;\frac{3}{2},2;\frac{1}{2}\big) + 2\sqrt{2e\pi}\big[\mathrm{erfc}\big(\frac{1}{\sqrt{2}}\big)-3\big] + 4\pi\,\mathrm{erfi}\big(\frac{1}{\sqrt{2}}\big) - 4\ln\big(\frac{2t}{\tau}\big) - 4\gamma_\mathrm{E} + 22}{8\sqrt{e\pi}}. \tag{74}$$

J. Order ε, third diagram $\mathbb{G}_\beta$

Using again the integral representation Eq. (71), the third diagram for the insertion of $\mathcal{S}_\beta$ is read off from Fig. 1 as

$$\begin{aligned}\tilde{\mathbb{G}}_\beta(m,s) &= \lim_{x_0\to 0}\frac{1}{x_0}\int_0^\Lambda \frac{dy}{y}\int_{x_1>0}\tilde{P}_+(m,x_1,s)\,\partial_{x_1}[\tilde{P}_+(x_1,x_0,s)e^{-\tau y} - \tilde{P}_+(x_1,x_0,s+y)]\\ &= \int_0^\infty dy\left[\frac{\sqrt{y+1}e^{-m\sqrt{s}}}{\sqrt{s}y^2} - \frac{\sqrt{y+1}e^{-m\sqrt{s}\sqrt{y+1}}}{\sqrt{s}y^2} - \frac{me^{-m\sqrt{s}-s\tau y}}{2y}\right]\\ &= \frac{e^{-m\sqrt{s}}\big\{m\sqrt{s}\big[2-\ln\big(\frac{m^2}{4s\tau^2}\big)\big]+\ln(4m^2s)+2\gamma_\mathrm{E}\big\}}{4\sqrt{s}} - \frac{e^{m\sqrt{s}}(m\sqrt{s}+1)\mathrm{Ei}(-2m\sqrt{s})}{2\sqrt{s}}.\end{aligned} \tag{75}$$

We checked that the y integrand is convergent, as it decays at least as $1/y^{3/2}$ for large y, and has a finite limit for $y\to 0$, thus no UV cutoff is necessary, and the y integral is finite.

Doing the inverse Laplace transform using Appendix C of Ref. [62], we get with z defined in Eq. (68)

$$\sqrt{t}\,\mathbb{G}_\beta(m,t) = \frac{e^{-\frac{z^2}{2}}[\mathcal{I}(z)-2]}{2\sqrt{\pi}(1-z^2)} + \frac{z\,\mathrm{erfc}\big(\frac{z}{\sqrt{2}}\big)}{\sqrt{2}(z^2-1)} + \frac{e^{-\frac{z^2}{2}}z^2\big[1-\ln\big(\frac{t}{\tau}\big)\big]}{2\sqrt{\pi}}. \tag{76}$$

K. Combinations

Let us remind that in the drift-free case the result for $\mathbb{G}_0(z)$ is given in Eq. (69), while $\mathbb{G}_1(z)$ is given in Eq. (70). Let us now turn to the corrections for drift. While $\mathbb{G}_\alpha$ and $\mathbb{G}_\beta$ are the appropriate functions for the calculations, we finally need the corrections for linear drift μ and nonlinear drift ν. Demanding that

$$\alpha\mathbb{G}_\alpha + \beta\mathbb{G}_\beta \stackrel{!}{=} \mu\mathbb{G}_\mu + \nu\mathbb{G}_\nu, \tag{77}$$

and using Eqs. (41) and (42) yields

$$\begin{aligned}\sqrt{t}\mathbb{G}_\mu(m,t) &= \sqrt{t}[\mathbb{G}_\alpha(m,t)+\mathbb{G}_\beta(m,t)]\\ &= -\frac{e^{-\frac{z^2}{2}}(z^2+1)[\mathcal{I}(z)-2]}{2\sqrt{\pi}(z^2-1)} + \frac{\sqrt{2}\,z\,\mathrm{erfc}(\frac{z}{\sqrt{2}})}{z^2-1} - \frac{e^{-\frac{z^2}{2}}z^2\big[\ln\big(\frac{2t^2z^2}{\tau^2}\big)+\gamma_\mathrm{E}-2\big]}{2\sqrt{\pi}},\end{aligned} \tag{78}$$

$$\sqrt{t}\mathbb{G}_\nu(m,t) = \sqrt{t}[\mathbb{G}_\beta(m,t)-\mathbb{G}_\alpha(m,t)] = \frac{e^{-\frac{z^2}{2}}[\mathcal{I}(z)-2]}{2\sqrt{\pi}} + \frac{e^{-\frac{z^2}{2}}z^2[\ln(2z^2)+\gamma_\mathrm{E}]}{2\sqrt{\pi}}. \tag{79}$$

The perturbative contributions can be grouped together as, cf. Eqs. (52) and (62)

$$\mathbb{G}(m,t) := \exp\left(-\frac{m}{2}\left[\frac{\mu}{D_\varepsilon}+\nu\right] - \frac{t}{4}[\mu t^{-\varepsilon}+\nu t^\varepsilon]^2\right)\big\{\mathbb{G}_0(m,t) + \varepsilon[\,\mathbb{G}_1(m,t) - \mu\,\mathbb{G}_\mu(m,t) - \nu\,\mathbb{G}_\nu(m,t)]\big\}. \tag{80}$$

This expression is to this order equivalent to

$$\mathbb{G}(m,t) := \exp\left(-\frac{m}{2}\left[\frac{\mu}{D_\varepsilon}+\nu\right] - \frac{t}{4}[\mu t^{-\varepsilon}+\nu t^\varepsilon]^2\right)\mathbb{G}_0(m,t)\exp\left(\varepsilon\frac{\mathbb{G}_1(m,t)-\mu\,\mathbb{G}_\mu(m,t)-\nu\,\mathbb{G}_\nu(m,t)}{\mathbb{G}_0(m,t)}\right). \tag{81}$$

See Ref. [63], Sec. IV C for a discussion of why it is better to write the perturbative corrections in an exponential form.

L. Scaling and corrections from the diffusion constant, final result

The natural scaling variable for fBm is not z, but

$$y := \frac{m}{\sqrt{2}t^H}. \tag{82}$$

This will induce some corrections [cf. Eq. (49)]. Consider

$$\frac{e^{-\frac{y^2}{2}}y}{\sqrt{2\pi}} = \frac{e^{-\frac{z^2}{2}}z}{\sqrt{2\pi}}[1+(z^2-1)\varepsilon\ln(t)] + \mathcal{O}(\varepsilon^2). \tag{83}$$

There is also a correction to the diffusion constant,

$$D_\varepsilon \simeq (e\tau)^{2\varepsilon}. \tag{84}$$

According to Eq. (49), this implies that

$$\begin{aligned}\mathbb{P}(m,t) &= \mathbb{G}(m,tD_\varepsilon)\\ &= \frac{e^{-\frac{y^2}{2}}y}{\sqrt{2\pi}tD_\varepsilon}\times\exp\left(-\frac{m}{2}\left[\frac{\mu}{D_\varepsilon}+\nu\right]\right)\\ &\quad\times\exp\left\{-\frac{D_\varepsilon t}{4}[\mu^2(D_\varepsilon t)^{-2\varepsilon}+\nu^2(D_\varepsilon t)^{2\varepsilon}]\right\}\\ &\quad\times\exp\left\{\varepsilon\left[\frac{\mathbb{G}_1(m,t)-\mu\,\mathbb{G}_\mu(m,t)-\nu\,\mathbb{G}_\nu(m,t)}{\mathbb{G}_0(m,t)}\right.\right.\\ &\quad\left.\left.-(y^2-1)\ln(t)\right]\right\}\end{aligned}\tag{85}$$

Note that we used the factored form Eq. (81) to make appear the ratios of $\mathbb{G}_1$, $\mathbb{G}_\mu$, and $\mathbb{G}_\nu$ with $\mathbb{G}_0$, yielding (relatively simple) special functions $\mathcal{F}_1$, $\mathcal{F}_\mu$, and $\mathcal{F}_\nu$ defined below. Regrouping terms yields

$$\begin{aligned}\mathbb{P}(m,t) &= \frac{e^{-\frac{y^2}{2}}y^{\frac{1}{H}-1}}{\sqrt{2\pi t}}\\ &\quad\times\exp\left(-\frac{\mu m^{1-2\varepsilon/H}}{2}y^{2\varepsilon}-\frac{\nu m}{2}y^{\varepsilon}\right.\\ &\quad\left.-\frac{t}{4}[\mu t^{-\varepsilon}+\nu t^{\varepsilon}]^2\right)\\ &\quad\times\exp(\varepsilon[\mathcal{F}_1(y)-\mu m\mathcal{F}_\mu(y)-\nu m\mathcal{F}_\nu(y)]).\end{aligned}\tag{86}$$

To order ε, this can be rewritten in a more intuitive form as

$$\begin{aligned}t\,\mathbb{P}(m,t) &= \frac{y^{\frac{1}{H}-1}}{\sqrt{2\pi}}\times\exp\left(-\frac{y^2}{2}+\varepsilon\left[\mathcal{F}_1(y)+\mathcal{F}_1^0\right]\right.\\ &\quad-\mu m^{\frac{1}{H}-1}y^{2\varepsilon}\left[\frac{1}{2}+\varepsilon\mathcal{F}_\mu(y)\right]\\ &\quad\left.-\nu m y^{2\varepsilon}\left[\frac{1}{2}+\varepsilon\mathcal{F}_\nu(y)\right]-\frac{m^2}{8y^2}\left[\mu\left(\frac{2y^2}{m^2}\right)^{\frac{\varepsilon}{H}}+\nu\right]^2\right).\end{aligned}\tag{87}$$

Note that since our expansion is restricted to the first order in ε, in expressions like

$$\frac{1}{H}-1=1-4\varepsilon+\mathcal{O}(\varepsilon^2),\quad 1-\frac{1}{2H}=2\varepsilon+\mathcal{O}(\varepsilon^2),\tag{88}$$

we have no means to distinguish between left- and right-hand side. Some choices are given by scaling, as the prefactor of $y^{\frac{1}{H}-1}$, or seem natural, others are educated guesses.

Finally, we wish to rewrite Eq. (87) (a density in time) as a density in y, given distance m from the absorbing boundary for the starting point. Using that

$$\frac{dt}{t}=\frac{1}{H}\frac{dy}{y},\tag{89}$$

this yields

$$\mathcal{P}(y|m,\mu,\nu)=\mathcal{P}_>(y|m,\mu,\nu)+\mathbf{P}_{\text{escape}}(m,\mu,\nu)\delta(y).\tag{90}$$

The function $\mathcal{P}_>(y|m,\mu,\nu)$ is equivalent to Eq. (87) after the change in measure Eq. (89),

$$\begin{aligned}\mathcal{P}_>(y|m,\mu,\nu) &= \frac{y^{\frac{1}{H}-2}}{\sqrt{2\pi}H}\\ &\quad\times\exp\left(-\frac{y^2}{2}+\varepsilon\left[\mathcal{F}_1(y)+\mathcal{F}_1^0\right]-\mu m^{\frac{1}{H}-1}y^{2\varepsilon}\left[\frac{1}{2}+\varepsilon F_\mu(y)\right]\right.\\ &\quad\left.-\nu m y^{2\varepsilon}\left[\frac{1}{2}+\varepsilon\mathcal{F}_\nu(y)\right]-\frac{m^2}{8y^2}\left[\mu\left(\frac{2y^2}{m^2}\right)^{\frac{\varepsilon}{H}}+\nu\right]^2\right).\end{aligned}\tag{91}$$

Some trajectories escape, which we count as absorption time $t=\infty$, equivalent to $y=0$, resulting into the contribution proportional to $\delta(y)$ in Eq. (90), with amplitude

$$\mathbf{P}_{\text{escape}}(m,\mu,\nu)=1-\mathbf{P}_{\text{abs}}(m,\mu,\nu),\tag{92}$$

where

$$\mathbf{P}_{\text{abs}}(m,\mu,\nu):=\int_0^\infty dy\,\mathcal{P}_>(y|m,\mu,\nu).\tag{93}$$

It is evaluated in the next section, see Eqs. (121)–(123).

The three special functions appearing in Eq. (86) and plotted on Fig. 2 are defined as follows: First, the drift-free contributions are

$$\begin{aligned}&\mathcal{F}_1(y)+\mathcal{F}_1^0\\ &:=\frac{\mathbb{G}_1(y)}{\mathbb{G}_0(y)}-(y^2-1)[\ln(t/\tau)-1]+4\ln y\\ &=\mathcal{I}(y)+y^2[\ln(2y^2)+\gamma_{\text{E}}]-2(\gamma_{\text{E}}+1+\ln 2).\end{aligned}\tag{94}$$

The conventions are s.t. $\mathcal{F}_1(y)$ agrees with Refs. [42,44,61], i.e., $\mathcal{F}_1(0)=0$. The constant part $\mathcal{F}_1^0$ is equivalent to a change in normalization, $\mathcal{N}=\exp(-\varepsilon\mathcal{F}_1^0)$, which for the drift-free case was of no interest [42,44,61], as there the absorption probability is one, which is not the case with drift. In the chosen convention (plotted on Fig. 2),

$$\mathcal{F}_1(y)=\mathcal{I}(y)+y^2[\ln(2y^2)+\gamma_{\text{E}}]-2,\tag{95}$$

$$\mathcal{F}_1(0)=0,\tag{96}$$

$$\mathcal{F}_1^0=-2(\gamma_{\text{E}}+\ln 2).\tag{97}$$

Its asymptotic expansions for small and large y are

$$\begin{aligned}\mathcal{F}_1(y) &= 2\sqrt{2\pi}y+y^2[\ln\left(2y^2\right)+\gamma_{\text{E}}-3]-\frac{1}{3}\sqrt{2\pi}y^3\\ &\quad+\frac{y^4}{6}-\frac{1}{30}\sqrt{\frac{\pi}{2}}y^5+\frac{y^6}{90}-\frac{1}{420}\sqrt{\frac{\pi}{2}}y^7+\frac{y^8}{1260}\\ &\quad-\frac{\sqrt{\frac{\pi}{2}}y^9}{6048}+\frac{y^{10}}{18900}+\mathcal{O}(y^{11}),\end{aligned}\tag{98}$$

$$\begin{aligned}\mathcal{F}_1(y) &= \ln(y^2/2)+1-\psi\left(\tfrac{1}{2}\right)+\frac{1}{2y^2}-\frac{1}{2y^4}+\frac{5}{4y^6}\\ &\quad-\frac{21}{4y^8}+\frac{63}{2y^{10}}+\mathcal{O}(y^{-11}).\end{aligned}\tag{99}$$

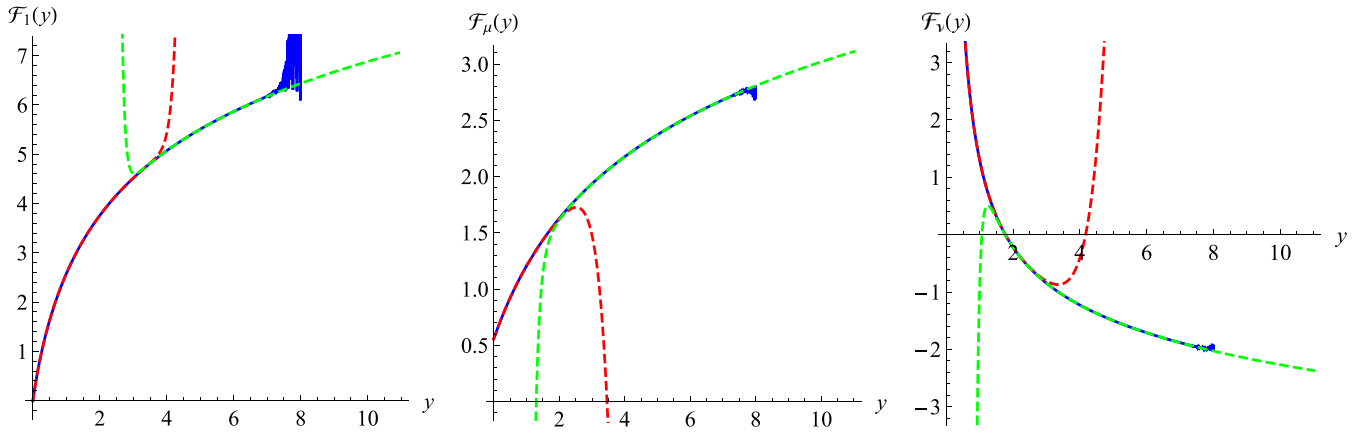

FIG. 2. Left: The function $\mathcal{F}_1(y)$ (blue, solid), with its asymptotic expansions (red and green dashed). Middle: same for $\mathcal{F}_\mu(y)$. Right: same for $\mathcal{F}_\nu(y)$. Numerical measurements are presented on Figs. 5, 6, and 8.

Equation (95) is equivalent to Eq. (55) in Ref. [61] and Eq. (56) in Ref. [42].

The second function is for the drift proportional to μ,

$$\mathcal{F}_\mu(y) := \frac{\mathbb{G}_\mu(m,t)}{m\mathbb{G}_0(m,t)} + \partial_\varepsilon\Big|_{\varepsilon=0}\left(\frac{m^{4\varepsilon}}{2D_\varepsilon y^{2\varepsilon}}\right). \tag{100}$$

It is evaluated as (for a plot see Fig. 2)

$$\mathcal{F}_\mu(y) = \frac{(y^2+1)[\mathcal{I}(y)-2]}{2y^2(1-y^2)} + \frac{\sqrt{2\pi}e^{\frac{y^2}{2}}\operatorname{erfc}\left(\frac{y}{\sqrt{2}}\right)}{y(y^2-1)} + \frac{1}{2}[\ln(2)-\gamma_{\mathrm{E}}]. \tag{101}$$

Its asymptotic expansions are

$$\mathcal{F}_\mu(y) = \frac{1}{2}[1-\gamma_{\mathrm{E}}+\ln(2)] + \frac{1}{3}\sqrt{2\pi}y - \frac{y^2}{4} + \frac{1}{15}\sqrt{\frac{\pi}{2}}y^3 - \frac{y^4}{36} + \frac{1}{140}\sqrt{\frac{\pi}{2}}y^5 - \frac{y^6}{360} + \frac{\sqrt{\frac{\pi}{2}}y^7}{1512} - \frac{y^8}{4200} + \frac{\sqrt{\frac{\pi}{2}}y^9}{19\,008} - \frac{y^{10}}{56\,700} + \mathcal{O}(y^{11}), \tag{102}$$

$$\mathcal{F}_\mu(y) = \ln(2y) + \frac{\ln(2y^2)+\gamma_{\mathrm{E}}-1}{2y^2} + \frac{3}{4y^4} - \frac{5}{4y^6} + \frac{35}{8y^8} - \frac{189}{8y^{10}} + \mathcal{O}(y^{-11}). \tag{103}$$

Note that we added some strangely looking factors into the result Eq. (91). The factor $m \times m^{-\frac{2\varepsilon}{H}} = m^{\frac{1}{H}-1}$ accounts for the dimension of the diffusion constant, $m/D_\varepsilon \sim m\tau^{-2\varepsilon}$, and takes out the term $\ln(m)$ from $\mathcal{F}_\mu(y)$. We moved out also a remaining term $\sim \ln y$.

The third function is for the drift proportional to ν,

$$\mathcal{F}_\nu(y) := \frac{\mathbb{G}_\nu(y)}{\mathbb{G}_0(y)m} - \ln(y). \tag{104}$$

It is evaluated as (for a plot see Fig. 2)

$$\mathcal{F}_\nu(y) = \frac{\mathcal{I}(y)-2}{2y^2} + \frac{\ln(2)+\gamma_{\mathrm{E}}}{2}. \tag{105}$$

Its asymptotic expansions read

$$\mathcal{F}_\nu(y) = \frac{\sqrt{2\pi}}{y} + \frac{-3+\gamma_{\mathrm{E}}+\ln(2)}{2} - \frac{1}{3}\sqrt{\frac{\pi}{2}}y + \frac{y^2}{12} - \frac{1}{60}\sqrt{\frac{\pi}{2}}y^3 + \frac{y^4}{180} - \frac{1}{840}\sqrt{\frac{\pi}{2}}y^5 + \frac{y^6}{2520} - \frac{\sqrt{\frac{\pi}{2}}y^7}{12096} + \frac{y^8}{37800} - \frac{\sqrt{\frac{\pi}{2}}y^9}{190080} + \frac{y^{10}}{623700} + \mathcal{O}(y^{11}), \tag{106}$$

$$\mathcal{F}_\nu(y) = -\ln(y) + \frac{2\ln(y)+\gamma_{\mathrm{E}}+1+\ln(2)}{2y^2} + \frac{1}{4y^4} - \frac{1}{4y^6} + \frac{5}{8y^8} - \frac{21}{8y^{10}} + \mathcal{O}(y^{-11}). \tag{107}$$

Using Eq. (91) for small y, there is a problem when $\varepsilon\nu < 0$, since then the combination (second-to-last term in the exponential)

$$-\varepsilon\nu m y^{2\varepsilon}\left[\tfrac{1}{2}+\varepsilon\mathcal{F}_\nu(y)\right] \xrightarrow{y\to 0} -\varepsilon\nu m\sqrt{2\pi}y^{2\varepsilon-1} \approx -2\nu\sqrt{\pi}t^H \tag{108}$$

diverges (at least for $\frac{1}{4} < H < \frac{1}{2}$), which is amplified since it appears inside the exponential. We propose to use the following Padé variant, which seems to work well numerically,

$$\left[\frac{1}{2}+\varepsilon\mathcal{F}_\nu(y)\right] \xrightarrow{\varepsilon<0,\,\nu>0} \frac{1}{2-4\varepsilon\mathcal{F}_\nu(y)}. \tag{109}$$

While $\mathcal{F}_\nu(y)$ diverges for small y, this is at leading order nothing but a normalization factor depending on νt^H.

All three functions $\mathcal{F}_1(y)$, $\mathcal{F}_\mu(y)$, and $\mathcal{F}_\nu(y)$ are measured in Sec. III; see Figs. 5, 6, and 8.

M. Absorption probability

From Eq. (62), we obtain $\mathbf{P}_{\mathrm{abs}}(m,\alpha,\beta)$,

$$\begin{aligned}\mathbf{P}_{\rm abs}(m,\alpha,\beta) &= \int_0^\infty dt\ \mathbb{G}(m,tD_\varepsilon)\\ &= \int_0^\infty dt\ \exp\!\left(-\frac{m}{2}\left[\frac{\mu}{D_\varepsilon}+\nu\right]-\frac{t}{4}[\mu t^{-\varepsilon}+\nu t^{\varepsilon}]^2\right)\mathbb{G}_0(m,tD_\varepsilon)\\ &\quad+\varepsilon\int_0^\infty dt\exp\!\left(-\frac{m}{2}\beta-\frac{t}{4}\beta^2\right)[\mathbb{G}_1(m,t)-\alpha\,\mathbb{G}_\alpha(m,t)-\beta\mathbb{G}_\beta(m,t)]+\mathcal{O}(\varepsilon^2)\\ &= \exp\!\left(-\frac{m}{2}\left[\frac{\mu}{D_\varepsilon}+\nu\right]\right)\left\{\int_0^\infty dt\ \exp\!\left(-\frac{t}{4}[\mu t^{-\varepsilon}+\nu t^{\varepsilon}]^2\right)\mathbb{G}_0(m,tD_\varepsilon)\right.\\ &\quad\left.+\ \varepsilon[\tilde{\mathbb{G}}_1(m,s)-\alpha\,\tilde{\mathbb{G}}_\alpha(m,s)-\beta\tilde{\mathbb{G}}_\beta(m,s)]\Big|_{\sqrt{s}=|\beta|/2}\right\}+\mathcal{O}(\varepsilon^2).\end{aligned}\tag{110}$$

Here $\tilde{\mathbb{G}}_1(m,s)$ is given by Eq. (65), $\tilde{\mathbb{G}}_\alpha(m,s)$ by Eq. (72), and $\tilde{\mathbb{G}}_\beta(m,s)$ by Eq. (75). We still need the integral

$$\begin{aligned}&\int_0^\infty dt\ \exp\!\left(-\frac{t}{4}[\mu t^{-\varepsilon}+\nu t^{\varepsilon}]^2\right)\mathbb{G}_0(m,tD_\varepsilon)\\ &\qquad= e^{-|\beta|m/(2\sqrt{D_\varepsilon})}+\frac{\alpha\beta}{2}\varepsilon\,\mathbb{G}_3(m,\beta),\end{aligned}\tag{111}$$

$$\mathbb{G}_3(m,\beta)=\int_0^\infty dt\,e^{-\frac{\beta^2 t}{4}}t\ln(t)\mathbb{G}_0(m,t).\tag{112}$$

The last expression can be calculated as

$$\begin{aligned}\mathbb{G}_3(m,\beta) &:= \int_0^\infty dt\,e^{-\frac{\beta^2 t}{4}}t\ln(t)\mathbb{G}_0(m,t)\\ &= \partial_\kappa\Big|_{\kappa=0}\int_0^\infty dt\,e^{-\frac{\beta^2 t}{4}}t^{1+\kappa}\mathbb{G}_0(m,t)\\ &= \partial_\kappa\Big|_{\kappa=0}\frac{|\beta|^{-\kappa-\frac12}m^{\kappa+\frac32}K_{\kappa-\frac12}\left(\frac{m|\beta|}{2}\right)}{\sqrt{\pi}}\\ &= -\frac{m^{3/2}\partial_\kappa\Big|_{\kappa=0}K_{\kappa-\frac12}\left(\frac{|\beta|m}{2}\right)}{\sqrt{\pi|\beta|}}+\frac{me^{-\frac{|\beta|m}{2}}\ln\left(\frac{m}{|\beta|}\right)}{|\beta|}\\ &= -\frac{me^{\frac{m|\beta|}{2}}\mathrm{Ei}(-m|\beta|)}{|\beta|}+\frac{me^{-\frac{m|\beta|}{2}}\ln\left(\frac{m}{|\beta|}\right)}{|\beta|}\\ &= \frac{m}{|\beta|}[-2\ln(|\beta|)-\gamma_{\rm E}]+\frac12 m^2[-2\ln(m)-\gamma_{\rm E}+2)]+\mathcal{O}(m^3),\end{aligned}\tag{113}$$

where $K_n(z)$ denotes the modified Bessel function of the second kind. With the above formulas, Eq. (110) is rewritten as

$$\begin{aligned}&\mathbf{P}_{\rm abs}(m,\alpha,\beta)\\ &\quad= e^{-m(\beta+|\beta|)/2}\left\{1+\varepsilon\,e^{|\beta|m/2}\left[\frac{\alpha\beta}{2}\mathbb{G}_3(m,\beta)\right.\right.\\ &\qquad+\frac{\alpha+\beta+|\beta|}{2}m(1+\ln\tau)e^{-|\beta|m/2}+\tilde{\mathbb{G}}_1(m,s)\\ &\qquad\left.\left.-\alpha\tilde{\mathbb{G}}_\alpha(m,s)-\beta\tilde{\mathbb{G}}_\beta(m,s)\right]\Big|_{\sqrt{s}=\frac{|\beta|}{2}}+\mathcal{O}(\varepsilon^2)\right\}.\end{aligned}\tag{114}$$

We note the exact relations, which can be verified numerically,

$$\tilde{\mathbb{G}}_1(m,s)+2\sqrt{s}\,\tilde{\mathbb{G}}_\beta(m,s)=0,\tag{115}$$

$$\mathbb{G}_3(m,\beta)|\beta|+2\tilde{\mathbb{G}}_\alpha(m,s)-m(1+\ln\tau)\mathrm{e}^{-\frac{m|\beta|}{2}}\Big|_{\sqrt{s}=\frac{|\beta|}{2}}=0.\tag{116}$$

Let us analyze $\mathbf{P}_{\rm abs}$ separately for $\beta<0$ and $\beta>0$, starting with the former. Using both cancelations in Eqs. (115) and (116), we find

$$\mathbf{P}_{\rm abs}(\alpha,\beta<0)=1+\mathcal{O}(\varepsilon^2).\tag{117}$$

Thus, there is no change in normalization for a drift toward the absorbing boundary. For $\beta>0$, we find again with the use of Eqs. (115) and (116),

$$\mathbf{P}_{\rm abs}(\alpha,\beta>0)=e^{-m\beta}\times\{1+\varepsilon[(\alpha+\beta)m(1+\ln\tau)+2e^{\beta m/2}(\tilde{\mathbb{G}}_1(m,s)-\alpha\tilde{\mathbb{G}}_\alpha(m,s))_{\sqrt{s}=\frac{\beta}{2}}]+\mathcal{O}(\varepsilon^2)\}.\tag{118}$$

For what follows, we note regularity of the combination $\mathrm{Ei}(-x)-\ln(x)-\gamma_{\rm E}$. We can write Eq. (118) as

$$\begin{aligned}\mathbf{P}_{\rm abs}(m,\alpha,\beta) &= e^{-m\beta}\times\{1+\varepsilon\,[(m(\beta-\alpha)+2)(e^{\beta m}\mathrm{Ei}(-m\beta)-\ln(\beta m)-\gamma_{\rm E})\\ &\quad-\alpha m(2\ln(\beta)+\gamma_{\rm E})+\beta m(2\ln(m)+\gamma_{\rm E})]+\mathcal{O}(\varepsilon^2)\}\\ &= e^{-m\beta}\times\{1+\varepsilon\,m[2(\beta-\alpha)\ln(\beta)-\gamma_{\rm E}(\alpha+3\beta)-2\beta+4\beta\ln(m)]+\mathcal{O}(\varepsilon^2)+\mathcal{O}(m^2\varepsilon)\}.\end{aligned}\tag{119}$$

As the asymptotic expansion in the last line shows, a common resummation is possible; passing to variables μ and ν, it reads

$$\mathbf{P}_{\rm abs}(m,\mu,\nu)=\exp(-m^{\frac{1}{H}-1}\mu\,[1+2(1-\gamma_{\rm E})\varepsilon]-m^{\frac{1}{H}-1}\nu(\mu+\nu)^{\frac{1}{H}-2}\,[1+2(1-2\gamma_{\rm E})\varepsilon])+\mathcal{O}(\varepsilon^2)+\mathcal{O}(m^2\varepsilon).\tag{120}$$

This formula represents the leading behavior of $\mathbf{P}_{\rm abs}(m,\mu,\nu)$ for small m; thus, terms of order $\mathcal{O}(m^2\varepsilon)$ could be neglected. Note that the (inverse) powers of H were chosen s.t. the resulting object is scale invariant. Expanding in ε leads back to Eq. (119).

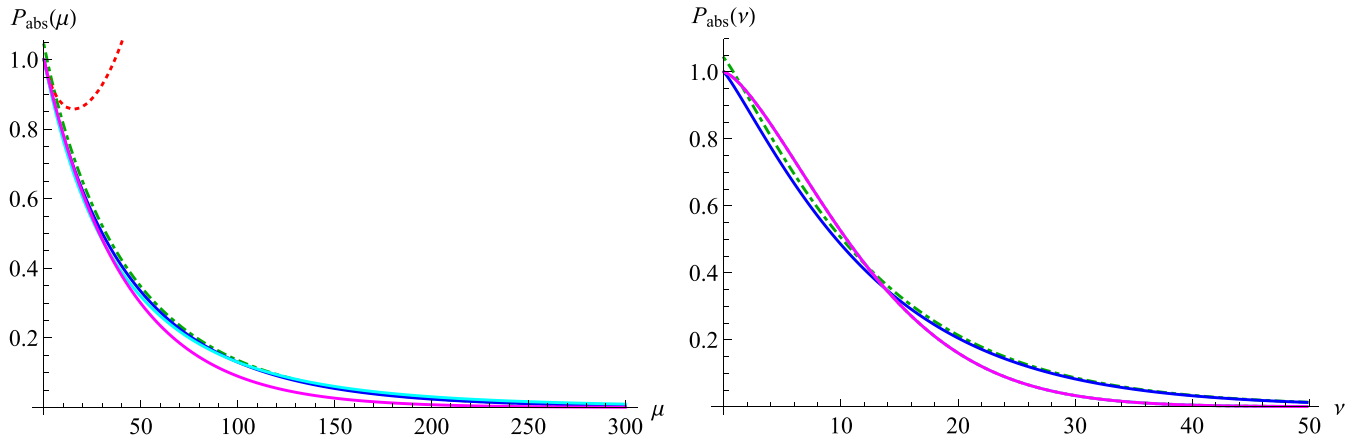

FIG. 3. Example for the absorption probability as a function of μ at $\nu = 0$ (left), and ν at $\mu = 0$ (right). In all cases $m = 0.1$. The blue solid line represents the result obtained by a direct numerical integration of Eq. (91), and adjusting the overall normalisation at $\mu = \nu = 0$ to 1; this has the advantage that the combination $\mu m^{\frac{1}{H}-1}$ appears naturally. The green dashed curve is the same, without adjustment of normalisation. The red dotted curve (visible only on the left plot) is obtained using Eq. (121). The magenta curve is obtained using Eq. (122). The cyan curve is from Eq. (123), and is identical to the magenta one on the right plot.

One finally arrives at (see Fig. 3)

$$\begin{aligned}\mathbf{P}_{\rm abs}(m,\mu,\nu) = \exp\big(&-m^{\frac{1}{H}-1}\{\mu\,[1+2(1-\gamma_{\rm E})\varepsilon]+\nu(\mu+\nu)^{\frac{1}{H}-2}[1+2(1-2\gamma_{\rm E})\varepsilon]\}\\&+\varepsilon\{2(m\nu+1)[e^{m(\mu+\nu)}{\rm Ei}(-m(\mu+\nu))-\ln(m(\mu+\nu))-\gamma_{\rm E}]\\&-2m(\mu+\nu)[\ln(m(\mu+\nu))+\gamma_{\rm E}-1]\}\big)+\mathcal{O}(\varepsilon^2).\end{aligned} \tag{121}$$

In order that this formula be invariant under $m \to \lambda m$, $\mu \to \lambda^{1-\frac{1}{H}}\mu$, and $\nu \to \lambda^{-1}\nu$, we can either replace $m\mu$ by $m\mu^{\frac{H}{1-H}}$, or $m^{\frac{1}{H}-1}\mu$. The first version is (see Fig. 3)

$$\begin{aligned}\mathbf{P}^{(a)}_{\rm abs}(m,\mu,\nu) = \exp\big(&-m^{\frac{1}{H}-1}\{\mu\,[1+2(1-\gamma_{\rm E})\varepsilon]+\nu(\mu^{\frac{H}{1-H}}+\nu)^{\frac{1}{H}-2}\,[1+2(1-2\gamma_{\rm E})\varepsilon]\}\\&+\varepsilon\{2(m\nu+1)[e^{m(\mu^{\frac{H}{1-H}}+\nu)}{\rm Ei}(-m(\mu^{\frac{H}{1-H}}+\nu))-\ln(m(\mu^{\frac{H}{1-H}}+\nu))-\gamma_{\rm E}]\\&-2m(\mu^{\frac{H}{1-H}}+\nu)[\ln(m(\mu^{\frac{H}{1-H}}+\nu))+\gamma_{\rm E}-1]\}\big)+\mathcal{O}(\varepsilon^2).\end{aligned} \tag{122}$$

The alternative second version is (see Fig. 3)

$$\begin{aligned}\mathbf{P}^{(b)}_{\rm abs}(m,\mu,\nu) = \exp\big(&-m^{\frac{1}{H}-1}\{\mu\,[1+2(1-\gamma_{\rm E})\varepsilon]+\nu(\mu^{\frac{H}{1-H}}+\nu)^{\frac{1}{H}-2}\,[1+2(1-2\gamma_{\rm E})\varepsilon]\}\\&+\varepsilon\{2(m\nu+1)[e^{m^{\frac{1}{H}-1}\mu+m\nu}{\rm Ei}(-m^{\frac{1}{H}-1}\mu-m\nu)-\ln(m^{\frac{1}{H}-1}\mu+m\nu)-\gamma_{\rm E}]\\&-(m^{\frac{1}{H}-1}\mu+m\nu)[\ln(m^{\frac{1}{H}-1}\mu+m\nu)+\gamma_{\rm E}-1]\}\big)+\mathcal{O}(\varepsilon^2).\end{aligned} \tag{123}$$

From the appearance of fractal powers of m and ν in Eq. (120), we suspect that both power series in $m\mu^{\frac{H}{1-H}}$ and $m^{\frac{1}{H}-1}\mu$ might appear. While numerical simulations could decide which version is a better approximation, only higher-order calculations would be able to settle the question.

N. Relation between the full propagator, first-passage times, and the distribution of the maximum

In this section, we demonstrate how the probability densities of three different observables follow from the same scaling function. This shows how our result can be used to find the probability distribution of both running maxima and first-passage times for fBM with linear and nonlinear drift.

Let us start with the drift-free case, $\mu = \nu = 0$.

(i) In Ref. [61] was calculated $\mathbb{P}_+(m,t)$, the *normalized* probability density to be at m, given t, when starting at x_0 close to 0 (in Ref. [61] this quantity is denoted $P_+(x,t)$ with $m = x$). While $\mathbb{P}_+$ is a density in m, and thus should be denoted P_+ (cf. Table I), it is the time derivative of a probability, see Eq. (129). This can be seen from its definition,

$$\mathbb{P}_+(m,t) := \frac{P_+(m,t|x_0)}{\int_0^\infty dm\, P_+(m,t|x_0)}, \tag{124}$$

and the asymptotic expansion at small x_0, (see, e.g., Ref. [61], Appendix C)

$$\int_0^\infty dm\, P_+(m,t|x_0) \sim x_0^{\frac{1}{H}-1}, \tag{125}$$

which implies that $\mathbb{P}_+(m,t)$ has dimension 1/time.

(ii) Here we consider the probability density to be absorbed at time t when starting at m. This is a first-passage time, with distribution $\mathbb{P}_{\rm first}(m,t)$.

(iii) Third, let the process start at 0, and consider the distribution of the max m, given a total time t, $P_{\max}(m,t)$, denoted by $P_H^T(m)$ (with $t=T$) in Ref. [42].

All three objects have a scaling form depending on the same variable $y=\frac{m}{\sqrt{2}t^H}$:

$$\mathbb{P}_{\rm first}(m,t)=\frac{H}{t}\mathcal{P}_{\rm first}(y)\,, \tag{126}$$

$$\mathbb{P}_{+}(m,t)=\frac{H}{t}\mathcal{P}_{+}(y), \tag{127}$$

$$P_{\max}(m,t)=\frac{1}{\sqrt{2}T^H}\mathcal{P}_{\max}(y). \tag{128}$$

The factors of H and $\sqrt{2}$ where chosen for later convenience. These objects are related. Denote $\mathbf{P}_{\rm surv}(m,t)$ the probability to start at $x=0$, and to survive in presence of an absorbing boundary at m up to time t. Note that $\mathbf{P}_{\rm surv}(m,t)$ is a probability, whereas $\mathbb{P}_{\rm first}(m,t)$, $\mathbb{P}_{+}(m,t)$, and $P_{\max}(m,t)$ are densities, the first two in t, the latter in m. Then

$$\mathbb{P}_{+}(m,t)=\mathbb{P}_{\rm first}(m,t)=-\partial_t\mathbf{P}_{\rm surv}(m,t), \tag{129}$$

$$P_{\max}(m,t)=\partial_m\mathbf{P}_{\rm surv}(m,t). \tag{130}$$

Since $\mathbf{P}_{\rm surv}(m,t)$ is a probability, it is scale free, and scaling implies that

$$\mathbf{P}_{\rm surv}(m,t)=\mathbf{P}_{\rm surv}\left(y=\frac{m}{\sqrt{2}t^H}\right). \tag{131}$$

Putting together Eqs. (129), (130), and (131) proves Eqs. (126)–(128), with

$$\mathcal{P}_{\rm first}(y)=\mathcal{P}_{+}(y)=y\mathbf{P}'_{\rm surv}(y), \tag{132}$$

$$\mathcal{P}_{\max}(y)=\mathbf{P}'_{\rm surv}(y). \tag{133}$$

The scaling functions appearing are *almost* the same, differing by (innocent looking) factors of t and H and a (noninnocent looking) factor of y. However, when changing to the measure in y, all of them become *identical*. The survival probability in absence of a drift is given in Eqs. (63) and (64) of Ref. [42].

Let us finally add drift. Then the survival probability $\mathbf{P}_{\rm surv}(y,\tilde{u},v)$ depends on three variables introduced in Eqs. (12)–(15), setting there $x\to m$. Since $\tilde{u}=m\mu^{\frac{H}{1-H}}$, and $v=\nu m$ are both constants multiplying m, we can write $\mathbf{P}_{\rm surv}(y,\tilde{u},v)=\mathbf{P}_{\rm surv}(y,m)$. Using Eqs. (129) and (130), we find

$$\begin{aligned}\mathbb{P}_{+}(m,t)=\mathbb{P}_{\rm first}(m,t)&=-\frac{d}{dt}\mathbf{P}_{\rm surv}(y,m)\\&=\frac{H}{t}\partial_y\mathbf{P}_{\rm surv}(y,m),\end{aligned} \tag{134}$$

$$\begin{aligned}P_{\max}(m,t)&=\frac{d}{dm}\mathbf{P}_{\rm surv}(y,m)\\&=\left[\frac{y}{m}\partial_y+\partial_m\right]\mathbf{P}_{\rm surv}(y,m).\end{aligned} \tag{135}$$

Passing to the measure in y, we obtain

$$\mathcal{P}_{+}(y,m)=\mathcal{P}_{\rm first}(y,m)=y\partial_y\mathbf{P}_{\rm surv}(y,m), \tag{136}$$

$$\mathcal{P}_{\max}(y,m)=\left[\partial_y+\frac{m}{y}\partial_m\right]\mathbf{P}_{\rm surv}(y,m). \tag{137}$$

This set of equations allows us to express $\mathcal{P}_{\max}(y,m)$ as an integral over $\mathcal{P}_{+}(y,m)=\mathcal{P}_{\rm first}(y,m)$.

O. Tail of the distribution

Piterbarg [66] states (Sec. 11.3, p. 85) that for a fBm defined on the interval [0,1], with $\langle x_1^2\rangle=1$, in the limit of $u\to\infty$,

$$\begin{aligned}&\mathbf{P}(\max_{0\leqslant t\leqslant 1}x_t>u)\\&\simeq\mathbf{\Psi}(u)\times\begin{cases}2 & , \quad H=1/2\\ 1 & , \quad H>1/2\\ \dfrac{\mathcal{H}_{2H}}{2H}2^{\frac{1}{2H}}u^{\frac{1}{H}-2} & , \quad H<1/2\end{cases},\end{aligned} \tag{138}$$

$$\mathbf{\Psi}(u):=\frac{1}{\sqrt{2\pi}u}\exp\left(-\frac{u^2}{2}\right)\simeq\frac{1}{\sqrt{2\pi}}\int_u^\infty\exp\left(-\frac{x^2}{2}\right)dx. \tag{139}$$

The estimate for $H<1/2$ seems to contain misprints: We find $\sigma(t):=\sqrt{\langle x_t^2\rangle}=1-H|1-t|$ (i.e., H instead of $2H$). Rescaling $t-1\to(t-1)\times 2^{\frac{1}{2H}}$ gives $\sigma(t)\to 1-H\times 2^{\frac{1}{2H}}\times|1-t|$, thus

$$\mathbf{P}(\max_{0\leqslant t\leqslant 1}x_t>u)\simeq\frac{\mathcal{H}_{2H}}{2^{\frac{1}{2H}}H}u^{\frac{1}{H}-2}\mathbf{\Psi}(u),\quad H<\frac{1}{2}. \tag{140}$$

Using the latter result, taking a derivative w.r.t. u, and passing to the measure in y, one obtains $\mathcal{P}(y)\equiv\mathcal{P}_{>}(y|m,\mu=\nu=0)\equiv\mathcal{P}_{\max}(y)$ (in terms of our variable y), in the limit of large y,

$$\mathcal{P}(y)\simeq\frac{e^{-\frac{y^2}{2}}}{\sqrt{2\pi}}\times\begin{cases}2 & , \quad H=1/2\\ 1 & , \quad H>1/2\\ \dfrac{\mathcal{H}_{2H}}{2^{\frac{1}{2H}}H}y^{\frac{1}{H}-2} & , \quad H<1/2\end{cases}. \tag{141}$$

The Pickands constant $\mathcal{H}_{2H}$ has ε-expansion [54]

$$\mathcal{H}_{2H}=1-2\gamma_{\rm E}\varepsilon+\mathcal{O}(\varepsilon)^2. \tag{142}$$

How is this consistent with Eq. (91)? Taylor-expanding the latter for large y yields

$$\begin{aligned}\mathcal{P}(y)\simeq 2\frac{e^{-y^2/2}}{\sqrt{2\pi}}\{1-[1+\gamma_{\rm E}+2\ln(y)+\ln(2)]\varepsilon\\+\mathcal{O}(\varepsilon^2)+o(y^0)\}.\end{aligned} \tag{143}$$

In Ref. [61] this was interpreted as $\mathcal{P}(y)\sim y^{-2\varepsilon}e^{-y^2/2}$. Equation (141) shows that this interpretation is incorrect. For large y, our expansion is almost the sum of the two contributions in

Eq. (141) for $H \neq 1/2$,

$$\mathcal{P}(y) \approx \frac{e^{-y^2/2}}{\sqrt{2\pi}}\left[1 + \frac{\mathcal{H}_{2H}}{2^{\frac{1}{2H}}H} y^{\frac{1}{H}-2} + \ldots\right]$$
$$\simeq 2\frac{e^{-y^2/2}}{\sqrt{2\pi}}\{1 - [1 + \gamma_E + 2\ln(y) - \ln(2)]\varepsilon + \mathcal{O}(\varepsilon^2) + \mathcal{O}(y^0)\}. \quad (144)$$

Note the difference in sign for the ln(2) term between Eqs. (143) and (144), showing that the guessed Eq. (144) slightly underestimates the amplitude for $\varepsilon < 0$.

III. NUMERICS

A. Simulation protocol

Fractional Brownian motion can be simulated with the classical Davis-Harte (DH) algorithm [18,67], whose algorithmic complexity (execution time) scales with system size N as $N \ln N$. Here we use the adaptive-bisection algorithm introduced and explained in Refs. [68,69]. For $H = 1/3$ its measured algorithmic complexity grows as $(\ln N)^3$, making it about 5000 times faster, and 10 000 times less memory consuming than DH for an effective grid size of $N = 2^{32}$.

To measure the functions $\mathcal{F}_1$, $\mathcal{F}_\mu$, and $\mathcal{F}_\nu$, which all depend on y only, we

(i) generate a (drift free) fBm x_t with $x_0 = 0$, of length N; the latter corresponds to a time $T = 1$,

(ii) add the drift terms to yield $z_t = x_t + \mu t + \nu t^{2H}$,

(iii) for given m, find the first time t, s.t. $z_t = m$,

(iv) evaluate $y = \frac{m}{\sqrt{2}t^H}$; add a point to the histogram of y.

This histogram misses values of $t > T = 1$, i.e. $y < \frac{m}{\sqrt{2}}$.

We checked the procedure for Brownian motion (with $\nu \to 0$), where

$$\mathcal{P}(y|m,\mu) = \sqrt{\frac{2}{\pi}}\, e^{-\frac{(\mu m + 2y^2)^2}{8y^2}}. \quad (145)$$

Note that this is a function of y and $m\mu$ only, so that we can write

$$\mathcal{P}(y|m\mu) = \sqrt{\frac{2}{\pi}} e^{-\frac{y^2}{2}} \times e^{-\frac{m\mu}{2}} e^{-\frac{(m\mu)^2}{8y^2}}. \quad (146)$$

For fBm, we measure $\mathcal{P}(y|m,\mu,\nu)$, and then extract $\mathcal{F}_1$, $\mathcal{F}_\mu$, and $\mathcal{F}_\nu$. First,

$$\mathcal{F}_1^\varepsilon(y|m) := \frac{1}{\varepsilon}\ln\left(\mathcal{P}(y|m) y^{2-\frac{1}{H}} e^{\frac{y^2}{2}}\right)|_{\mu=\nu=0} \quad (147)$$

and $\mathcal{F}_1^\varepsilon(y|m) = \mathcal{F}_1(y) + \mathcal{O}(\varepsilon^2)$. The following combination is more precise, since terms even in ε cancel,

$$\mathcal{F}_1^{\varepsilon,\mathrm{sym}}(y|m) = \frac{1}{2}\left[\mathcal{F}_1^\varepsilon(y|m) + \mathcal{F}_1^{-\varepsilon}(y|m)\right] + \mathcal{O}(\varepsilon^2). \quad (148)$$

The second-order correction can be estimated as

$$\mathcal{F}_2^\varepsilon(y|m) := \frac{1}{\varepsilon}\left[\mathcal{F}_1^\varepsilon(y|m) - \mathcal{F}_1(y|m)\right] + \mathcal{O}(\varepsilon). \quad (149)$$

Its symmetrized version again suppresses subleading corrections,

$$\mathcal{F}_2^{\varepsilon,\mathrm{sym}}(y|m) := \frac{1}{2\varepsilon}\left[\mathcal{F}_1^\varepsilon(y|m) - \mathcal{F}_1^{-\varepsilon}(y|m)\right] + \mathcal{O}(\varepsilon^2). \quad (150)$$

The third-order correction can be extracted as

$$\mathcal{F}_3^\varepsilon(y|m) := \frac{1}{2\varepsilon^2}\left[\mathcal{F}_1^\varepsilon(y|m) + \mathcal{F}_1^{-\varepsilon}(y|m) - 2\mathcal{F}_1(y|m)\right] + \mathcal{O}(\varepsilon). \quad (151)$$

For the remaining functions $\mathcal{F}_\mu$ and $\mathcal{F}_\nu$, we can employ similar formulas; we have to decide how to subtract $\mathcal{F}_1$, numerically from the simulation, or analytically, i.e., by supplying numerically or analytically the denominator in

$$\mathcal{F}_\mu^\varepsilon(y|m,\mu) := -\frac{1}{\varepsilon}\left[\ln\left(\frac{\mathcal{P}(y|m,\mu,\nu=0)}{\mathcal{P}(y|m,\mu=\nu=0)}\right) \times \frac{y^{-2\varepsilon}}{\mu m^{\frac{1}{H}-1}} + \frac{1}{2} + \frac{\mu}{4}\left(\frac{m}{2}\right)^{\frac{1}{H}-1} y^{3-\frac{5}{2H}}\right], \quad (152)$$

$$\mathcal{F}_\nu^\varepsilon(y|m) := -\frac{1}{\varepsilon}\left[\ln\left(\frac{\mathcal{P}(y|m,\mu=0,\nu)}{\mathcal{P}(y|m,\mu=\nu=0)}\right) \times \frac{y^{-2\varepsilon}}{\nu m} + \frac{1}{2} + \frac{\nu m}{8} y^{-\varepsilon-2}\right]. \quad (153)$$

We can also work symmetrically

$$\mathcal{F}_\mu^\varepsilon(y|m) := -\frac{1}{\varepsilon}\left[\ln\left(\frac{\mathcal{P}(y|m,\mu,\nu=0)}{\mathcal{P}(y|m,-\mu,\nu=0)}\right)\frac{y^{-2\varepsilon}}{2\mu m^{\frac{1}{H}-1}} + \frac{1}{2}\right], \quad (154)$$

$$\mathcal{F}_\nu^\varepsilon(y|m) := -\frac{1}{\varepsilon}\left[\ln\left(\frac{\mathcal{P}(y|m,\mu=0,\nu)}{\mathcal{P}(y|m,\mu=0,-\nu)}\right)\frac{y^{-2\varepsilon}}{2\nu m} + \frac{1}{2}\right]. \quad (155)$$

Finally, a more precise estimate of the theoretical curves is given by symmetrizing results for the same $|\varepsilon|$, using the analog of Eq. (148).

Below, we measure the three scaling functions $\mathcal{F}_1$, $\mathcal{F}_\mu$, and $\mathcal{F}_\nu$ for $H = 0.33$, using our recently introduced adaptive-bisection algorithm [68,69]. The latter starts out with an initial coarse grid of size 2^g, which is then recursively refined up to a final gridsize of 2^{g+G}. It gains its efficiency by only sampling *necessary points*, i.e., those close to the target.

The optimal values of g and G depend on H. We run simulations with the following choices: $H = 0.33$ ($g = 8$, $G = 18$), $H = 0.4$ ($g = 10$, $G = 14$), $H = 0.6$ ($g = 8$, $G = 8$), and $H = 0.67$ ($g = 8$, $G = 6$). Thanks to the adaptive-bisection algorithm, we can maintain a resolution in x of 10^{-3}, with about 25 million samples at $H = 0.33$, $H = 0.6$, and $H = 0.67$, and twice as much for $H = 0.4$. As we will see below, this allows us to precisely validate our analytical predictions.

B. Simulation results

We show simulation results on Figs. 4 to 8. First, on Fig. 4 (left), we present results for the first-passage probability $\mathcal{P}(y|m,\mu,\nu=0)$, using $m = 0.1$. The numerical results (in color) are compared to the predictions from Eq. (91). One sees that theory and simulations are in good quantitative agreement. This comparison is made more precise by plotting the ratio between simulation and theory on the right of Fig. 4.

The function $\mathcal{F}_1(y)$ is extracted on Fig. 5. We show simulations for $m = 0.1$ (colored solid lines), and $m = 1$ (colored dashed lines). The theoretical result Eq. (95) agrees with

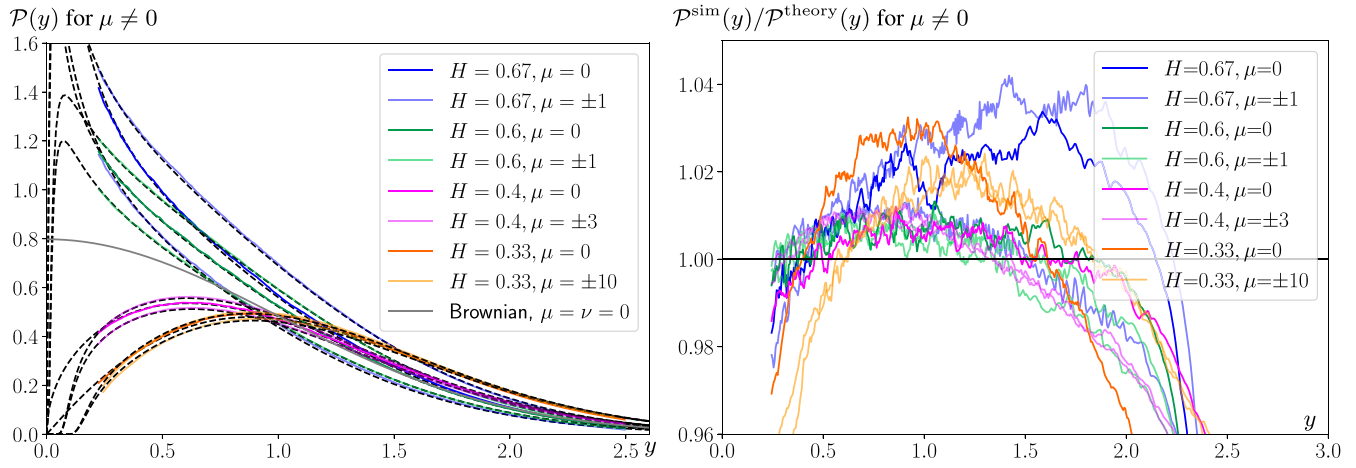

FIG. 4. Left: First-passage time density $\mathcal{P}_{\rm first}(m,t) = \mathcal{P}(y)$ plotted as a function of y as given in Eq. (9). To increase the resolution of the plot, we use overlapping bins with binsize 5×10^5, with y increasing by 10^5 points for each bin; $m = 0.1$. For various values of H and μ, numerical simulations are compared to the theory. As can be seen on this plot, and on the ratio between simulations and theory to the right, the relative error is about 3% at the extreme points. Note that neglecting $\mathcal{F}_1(y)$ would lead for $H = 0.4/0.6$ to an error of 15%, and for $H = 0.33/0.67$ to an error of 25%.

numerical simulations for all H, at both values of m. Using the symmetrized form Eq. (148) with $H = 0.4/0.6$ shows a particularly good agreement. It allows us to extract the subleading correction via Eqs. (149) and (150). This is shown in the inset of Fig. 5; again the symmetrized estimate is the most precise. Note that the second-order correction is rather sensitive to the choice of m; more effort would be needed to estimate it properly. Also note that adding a constant to $\mathcal{F}_1(y)$ is equivalent to an overall change in normalization, thus one should concentrate on the shape of the cuves.

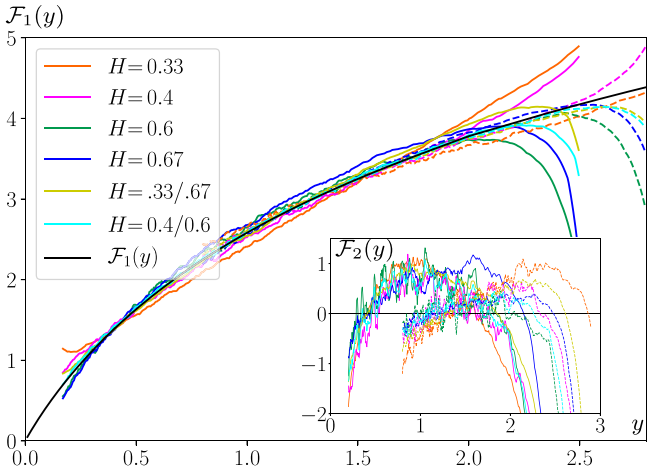

FIG. 5. Numerical estimate of $\mathcal{F}_1$. The black curve is the theoretical estimate Eq. (95), followed by a number of estimates using Eq. (147). Solid lines are for $m = 0.1$, dashed ones for $m = 1$. The symmetrized estimates Eq. (148) are in olive/cyan. The latter has minimal deviations from the theory. The inset shows a numerical estimate for $\mathcal{F}_2(y)$, as given by Eqs. (149) and (150). All curves are consistent, and let appear even the next-to-leading corrections. [Remember that changing the normalization is equivalent to adding a constant to $\mathcal{F}_1(y)$ or $\mathcal{F}_2(y)$.] The strong curve-down for small and large y are due to numerical problems.

Using the data presented on Fig. 4, Fig. 6 shows the order-ε correction $\mathcal{F}_\mu$ extracted via Eq. (154). The symmetrized estimate is rather close to the analytical result. The inset estimates the subleading correction. Again, estimates for $m = 0.1$ (dashed lines) and $m = 1$ (solid lines) are consistent, and a proper measure of the second-order correction would demand a higher numerical precision.

The results for nonlinear drift ν are presented on Fig. 7, starting with the probability distribution $\mathcal{P}(y|m)$ (left), followed by the ratio between simulation and theory on the right, using $m = 0.1$. The agreement is again good. From these

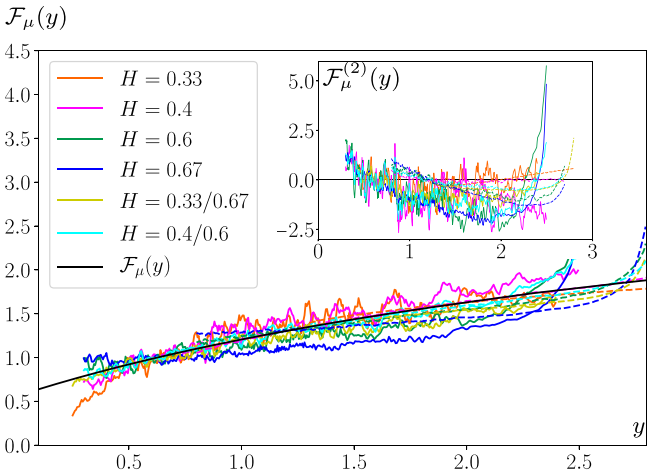

FIG. 6. Numerical estimate of $\mathcal{F}_\mu$. The black curve is the theoretical result Eq. (101). The colored curves are obtained using Eq. (154) with $\mu = \pm 1$ for $H = 0.6$ and $H = 0.67$, and $\mu = \pm 3$ for $H = 0.33$ and $H = 0.4$. Solid lines are for $m = 0.1$, dashed ones for $m = 1$. The symmetrized estimates Eq. (148) are in olive/cyan. The cyan curve using the equivalent of Eq. (148) with $H = 0.4/0.6$ is our best numerical estimate of $\mathcal{F}_\mu(y)$. The inset shows the estimated second-order correction, analogous to Eqs. (149) and (150).

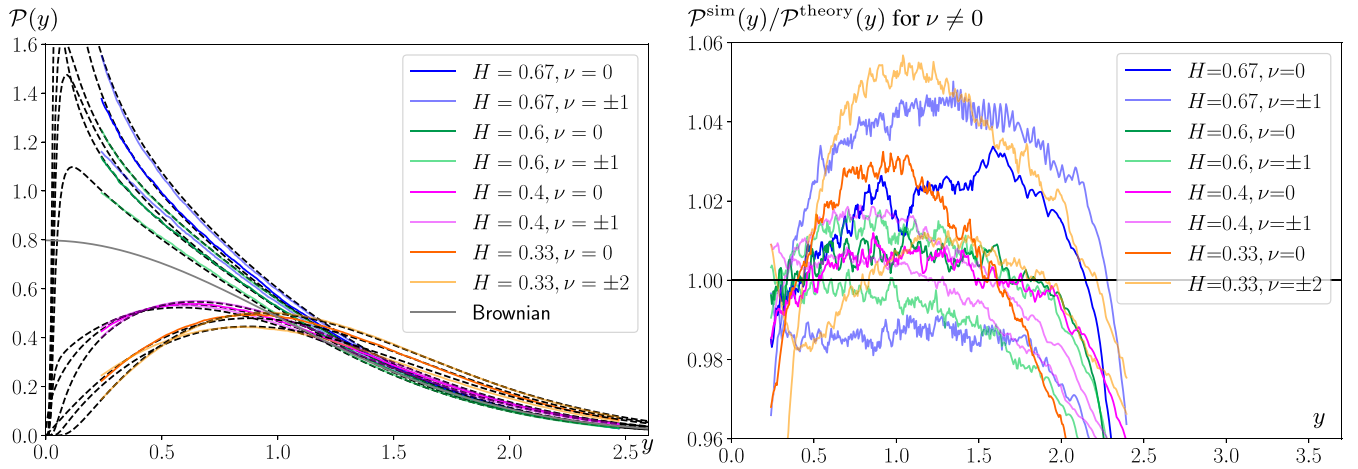

FIG. 7. Left: first-passage-time density plotted with overlapping bins as in Fig. 4 for various values of H and nonlinear drift ν compared to the theory given in Eq. (91). Right: Ratio of simulation and theoretical values.

data is extracted the function $\mathcal{F}_\nu(y)$ defined in Eq. (105), see Fig. 8. Note that $\mathcal{F}_\nu(y)$ is much larger than $\mathcal{F}_\mu(y)$ (Fig. 6), and diverges for small y. The subleading corrections to $\mathcal{F}_\nu(y)$ are not negligible, *seemingly* m-dependent, and estimated as well, allowing us to collapse all measured estimates on the theoretical curve.

In summary, we have measured all scaling functions with good to excellent precision, ensuring that the analytical results are correct.

IV. CONCLUSION

In this article, we gave analytical results for fractional Brownian motion, both with a linear and a nonlinear drift. Thanks to a novel simulation algorithm, we were able to verify the analytical predictions with grid sizes up to $N = 2^{28}$, leading to a precise validation of our results.

Our predictions to first order in $H - 1/2$ are precise, and many samples of very large systems are needed to see statistically significant deviations. We therefore hope that our formulas will find application in the analysis of data, as, e.g., the stock market.

Another interesting question is how a trajectory depends on its history, i.e. prior knowledge of the process. We obtained analytical results also in this case, and will come back with its numerical validation in future work.

Our study can be generalized in other directions, as, e.g., making the variance a stochastic process, as in [70] or in the rough-volatility model of Ref. [71], which both use fBm in their modeling.

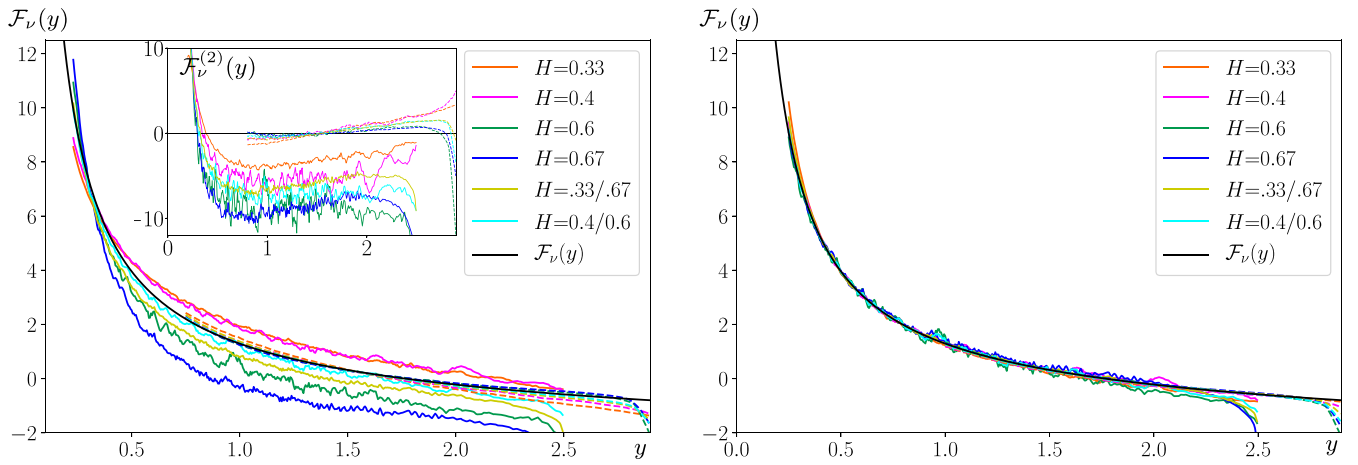

FIG. 8. Left: Numerical estimate of $\mathcal{F}_\nu$, using Eq. (155). The black curve is the theoretical prediction Eq. (105). The colored curves are simulation results using Eq. (155). Solid lines are for $m = 0.1$, dashed ones for $m = 1$. The cyan and olive curves are the symmetrized results using the equivalent of Eq. (148) for $H = 0.4/0.6$ (cyan) and $H = 0.33/0.67$ (olive). The former one is the best numerical estimate of the theory, and very close to the latter. The inset shows the estimated second-order corrections, analogous to Eqs. (149) and (150). There seem to be nonnegligible corrections of order three. An almost perfect data collapse can be obtained for $m = 0.1$ as $\varepsilon \mathcal{F}_\nu^\varepsilon(y) \simeq \mathcal{F}_\nu(y)\varepsilon + (2y^{-2} - 4y^{-1} - 6 + y)\varepsilon^2 + (3y - 20)\varepsilon^3$, and for $m = 1$ as $\varepsilon \mathcal{F}_\nu^\varepsilon(y) \simeq \mathcal{F}_\nu(y)\varepsilon + (y - 1.7)(1.5\varepsilon^2 - 6\varepsilon^3)$, see right figure. Since extrapolation problems mentioned around Eq. (109) become important for small y, this estimate is intended as a fit only, to show that the scatter on the left plot is consistent with higher-order corrections.

ACKNOWLEDGMENTS

It is a pleasure to thank J. P. Bouchaud and F. Gorokhovik for discussions, G. Pruessner for help with the implementation, and M. T. Jaekel and A. Thomas for support with the cluster. B.W. thanks Laboratoire de Physique Théorique de l'Ecole Normale Supérieure and Laboratoire de Physique de l'Ecole Normale Supérieure for hospitality.

[1] S. N. Majumdar, G. Schehr, and G. Wergen, Record statistics and persistence for a random walk with a drift, J. Phys. A **45**, 355002 (2012).

[2] G. Wergen, M. Bogner, and J. Krug, Record statistics for biased random walks, with an application to financial data, Phys. Rev. E **83**, 051109 (2011).

[3] P. Le Doussal and K. J. Wiese, Driven particle in a random landscape: Disorder correlator, avalanche distribution and extreme value statistics of records, Phys. Rev. E **79**, 051105 (2009).

[4] A. Rej, P. Seager, and J.-P. Bouchaud, You are in a drawdown. When should you start worrying? Wilmott **2018**, 26 (2018)

[5] N. Shome, C. A. Cornell, P. Bazzurro and J. E. Carballo, Earthquakes, records, and nonlinear responses, Earthquake Spectra **14**, 469 (1998).

[6] S. Redner, *A Guide to First-Passage Problems* (Cambridge University Press, Cambridge, UK, 2001).

[7] E. J. Gumbel, *Statistics of Extremes* (Dover, Oxford, UK, 1958).

[8] W. Feller, *Introduction to Probability Theory and Its Applications* (John Wiley & Sons, New York, 1950).

[9] W. Feller, *Introduction to Probability Theory and Its Applications*, Vol. 2 (John Wiley & Sons, New York, 1969).

[10] A. N. Borodin and P. Salminen, *Handbook of Brownian Motion—Facts and Formulae* (Birkhäuser, Basel, 2002).

[11] J. Bertoin, *Lévy Processes* (Cambridge University Press, Cambridge, UK, 1998).

[12] K. J. Wiese, Span observables—"When is a foraging rabbit no longer hungry?" J. Stat. Phys. **178**, 625 (2019).

[13] I. Nourdin, *Selected Aspects of Fractional Brownian Motion* (Bocconi & Springer Series, Berlin, 2012).

[14] T. Sottinen, Fractional Brownian motion, random walks and binary market models, Finance Stochast. **5**, 343 (2001).

[15] Y. G. Sinai, Distribution of the maximum of a fractional Brownian motion, Russian Math. Surveys **52**, 359 (1997).

[16] B. B. Mandelbrot and J. W. Van Ness, Fractional Brownian motions, fractional noises and applications, SIAM Rev. **10**, 422 (1968).

[17] J. Krug, Persistence of non-Markovian processes related to fractional Brownian motion, Markov Processes Relat. Fields **4**, 509 (1998).

[18] A. B. Dieker, Simulation of fractional Brownian motion, Ph.D. thesis, University of Twente, 2004.

[19] A. B. Dieker and M. Mandjes, On spectral simulation of fractional brownian motion, Probabil. Eng. Info. Sci. **17**, 417 (2003).

[20] F. Aurzada, On the one-sided exit problem for fractional Brownian motion, Electron. Commun. Probab. **16**, 392 (2011).

[21] L. Decreusefond and A. S. Üstünel, Fractional Brownian motion: Theory and applications, ESAIM: Proc. **5**, 75 (1998)

[22] P. L. Krapivsky, K. Mallick, and T. Sadhu, Dynamical properties of single-file diffusion, J. Stat. Mech. (2015) P09007.

[23] T. Sadhu and B. Derrida, Large deviation function of a tracer position in single file diffusion, J. Stat. Mech. (2015) P09008.

[24] T. Sadhu and B. Derrida, Correlations of the density and of the current in non-equilibrium diffusive systems, J. Stat. Mech. (2016) 113202.

[25] A. Zoia, A. Rosso and S. N. Majumdar, Asymptotic Behavior of Self-Affine Processes in Semi-Infinite Domainss, Phys. Rev. Lett. **102**, 120602 (2009).

[26] J. L. A. Dubbeldam, V. G. Rostiashvili, A. Milchev and T. A. Vilgis, Fractional Brownian motion approach to polymer translocation: The governing equation of motion, Phys. Rev. E **83**, 011802 (2011).

[27] V. Palyulin, T. Ala-Nissila and R. Metzler, Polymer translocation: The first two decades and the recent diversification, Soft Matter **10**, 9016 (2014).

[28] J.-P. Bouchaud and A. Georges, Anomalous diffusion in disordered media: statistical mechanisms, models and physical applications, Phys. Rep. **195**, 127 (1990).

[29] E. E. Peters, *Chaos and Order in the Capital Markets*, 2nd ed., Wiley finance editions (Wiley, New York, 1996).

[30] N. J. Cutland, P. E. Kopp and W. Willinger, Stock price returns and the Joseph effect: A fractional version of the Black-Scholes model, edited by E. Bolthausen, M. Dozzi, and F. Russo, in *Seminar on Stochastic Analysis, Random Fields and Applications*, Progress in Probability Vol. 36 (Birkhäuser Basel, 1995), pp. 327–351.

[31] F. Biagini, Y. Hu, B. Oksendal and T. Zhang, *Stochastic Calculus for Fractional Brownian Motion and Applications* (Springer Verlag, London, 2008).

[32] B. B. Mandelbrot and J. R. Wallis, Noah, Joseph, and operational hydrology, Water Resour. Res **4**, 909 (1968).

[33] S. Gupta, A. Rosso and C. Texier, Dynamics of a Tagged Monomer: Effects of Elastic Pinning and Harmonic Absorption, Phys. Rev. Lett. **111**, 210601 (2013).

[34] E. Monte-Moreno and M. Hernández-Pajares, Occurrence of solar flares viewed with gps: Statistics and fractal nature, J. Geophys. Res. A **119**, 9216 (2014).

[35] I. Simonsen, Measuring anti-correlations in the nordic electricity spot market by wavelets, Physica A **322**, 597 (2003).

[36] I. Norros, On the use of fractional Brownian motion in the theory of connectionless networks, IEEE J. Sel. Areas Commun. **13**, 953 (2006).

[37] K. Burnecki, E. Kepten, J. Janczura, I. Bronshtein, Y. Garini, and A. Weron, Universal algorithm for identification of fractional Brownian motion. A case of telomere subdiffusion, Biophys J. **103**, 1839 (2012).

[38] D. Ernst, M. Hellmann, J. Kohler and M. Weiss, Fractional Brownian motion in crowded fluids, Soft Matter **8**, 4886 (2012).

[39] J.-H. Jeon, A. V. Chechkin and R. Metzler, First passage behavior of fractional Brownian motion in two-dimensional wedge domains, Europhys. Lett. **94**, 20008 (2011).

[40] J.-H. Jeon, A. V. Chechkin, and R. Metzler, First passage behavior of multi-dimensional fractional Brownian motion and application to reaction phenomena, in *First-Passage Phenomena and Their Applications*, edited by R. Metzler, G.

Oshanin, and S. Redner (World Scientific, Singapore, 2013), pp. 175–202.

[41] T. Guérin, N. Levernier, O. Bénichou and R. Voituriez, Mean first-passage times of non-Markovian random walkers in confinement, Nature **534**, 356 (2016).

[42] M. Delorme and K. J. Wiese, Perturbative expansion for the maximum of fractional Brownian motion, Phys. Rev. E **94**, 012134 (2016).

[43] M. Delorme, Stochastic processes and disordered systems, around Brownian motion, Ph.D. thesis, PSL Research University (2016).

[44] M. Delorme and K. J. Wiese, Maximum of a Fractional Brownian Motion: Analytic Results from Perturbation Theory, Phys. Rev. Lett. **115**, 210601 (2015).

[45] K. Es-Sebaiy, I. Ouassou and Y. Ouknine, Estimation of the drift of fractional Brownian motion, Stat. Probab. Lett. **79**, 1647 (2009).

[46] F. Black and M. Scholes, The pricing of options and corporate liabilities, J. Political Econ. **81**, 637 (1973).

[47] J.-P. Bouchaud and M. Potters, *Theory of Financial Risk and Derivative Pricing* (Cambridge University Press, Cambridge, UK, 2009).

[48] M. Kardar, G. Parisi and Y.-C. Zhang, Dynamic Scaling of Growing Interfaces, Phys. Rev. Lett. **56**, 889 (1986).

[49] K. J. Wiese, On the perturbation expansion of the KPZ-equation, J. Stat. Phys. **93**, 143 (1998).

[50] H. K. Janssen, U. C. Tauber, and E. Frey, Exact results for the Kardar-Parisi-Zhang equation with spatially correlated noise, Eur. Phys. J. B **9**, 491 (1999).

[51] E. Hopf, The partial differential equation $u_t + uu_x = \mu_{xx}$, Commun. Pure Appl. Math. **3**, 201 (1950).

[52] J. D. Cole, On a quasi-linear parabolic equation occurring in aerodynamics, Q. Appl. Math. **9**, 225 (1951).

[53] K. Dębicki and P. Kisowski, A note on upper estimates for Pickands constants, Stat. Probab. Lett. **78**, 2046 (2008).

[54] M. Delorme, A. Rosso, and K. J. Wiese, Pickands' constant at first order in an expansion around Brownian motion, J. Phys. A **50**, 16LT04 (2017).

[55] L. de Haan and J. Pickands, Stationary min-stable processes, Probab. Theory Relat. Fields **72**, 477 (1986).

[56] A. J. Harper, Pickands' constant $\mathcal{H}_\alpha$ does not equal $1/\Gamma(1/\alpha)$, for small α, Bernoulli **23**, 582 (2017).

[57] Z. Michna, Remarks on Pickands theorem, Probab. Math. Stat. **37**, 373 (2017).

[58] J. Pickands III, Asymptotic properties of the maximum in a stationary Gaussian process, Trans. Amer. Math. Soc. **145**, 75 (1969).

[59] J. Pickands, The two-dimensional Poisson process and extremal processes, J. Appl. Probab. **8**, 745 (1971).

[60] J. Pickands, Statistical inference using extreme order statistics, Ann. Statist. **3**, 119 (1975).

[61] K. J. Wiese, S. N. Majumdar, and A. Rosso, Perturbation theory for fractional Brownian motion in presence of absorbing boundaries, Phys. Rev. E **83**, 061141 (2011).

[62] M. Delorme and K. J. Wiese, Extreme-value statistics of fractional Brownian motion bridges, Phys. Rev. E **94**, 052105 (2016).

[63] K. J. Wiese, First passage in an interval for fractional Brownian motion, Phys. Rev. E **99**, 032106 (2018).

[64] T. Sadhu, M. Delorme, and K. J. Wiese, Generalized Arcsine Laws for Fractional Brownian Motion, Phys. Rev. Lett. **120**, 040603 (2018).

[65] L. Benigni, C. Cosco, A. Shapira, and K. J. Wiese, Hausdorff dimension of the record set of a fractional Brownian motion, Electron. Commun. Probab. **23**, 1 (2018).

[66] V. I. Piterbarg, *Twenty Lectures About Gaussian Processes* (Atlantic Financial Press, London/New York, 2015).

[67] R. B. Davies and D. S. Harte, Tests for hurst effect, Biometrika **74**, 95 (1987).

[68] B. Walter and K. J. Wiese, Monte Carlo sampler of first-passage times for fractional Brownian motion using adaptive bisections: Source code, hal-02270046 (2019), https://hal.archives-ouvertes.fr/hal-02270046.

[69] B. Walter and K. J. Wiese, Sampling first-passage times of fractional Brownian motion using adaptive bisections, Phys. Rev. E **101**, 043312 (2020).

[70] F. Comte and E. Renault, Long memory in continuous-time stochastic volatility models, Math. Financ. **8**, 291 (1998).

[71] J. Gatheral, T. Jaisson, and M. Rosenbaum, Volatility is rough, Quant. Finance **18**, 933 (2018).